8 Soil Gas Movement in Unsaturated Systems

Bridget R. Scanlon, Jean Phillippe Nicot, and Joel W. Massmann

8.1 GENERAL CONCEPTS RELATED TO GAS MOVEMENT

An understanding of gas transport in unsaturated media is important for evaluation of soil aeration or movement of O_2 from the atmosphere to the soil. Soil aeration is critical for plant root growth because roots generally cannot get enough O_2 from leaves. Evaluation of gas movement is also important for estimating transport of volatile and semivolatile organic compounds from contaminated sites through the unsaturated zone to the groundwater. The use of soil venting, or soil vapor extraction, as a technique for remediating contaminated sites has resulted in increased interest in gas transport in the unsaturated zone (Rathfelder et al., 1995). Migration of gases from landfills, such as methane formed by decomposition of organic material, is important in many areas (Moore et al., 1982; Thibodeaux et al., 1982). Soil gas composition has also been used as a tool for mineral and petroleum exploration and for mapping organic contaminant plumes. An understanding of gas transport is important for evaluating movement of volatile radionuclides, such as ^{3}H, ^{14}C and Rd from radioactive waste disposal facilities. The adverse health effects of radon and its decay products have led to evaluation of transport in soils and into buildings (Nazaroff, 1992). A thorough understanding of gas transport is required to evaluate these issues.

Gas in the unsaturated zone is generally moist air, but it has higher CO_2 concentrations than atmospheric air because of plant root respiration and microbial degradation of organic compounds. Oxygen concentrations are generally inversely related to CO_2 concentrations because processes producing CO_2 generally deplete O_2 levels. Contaminated sites may have gas compositions that differ markedly from atmospheric air, depending on the type of contaminants.

This chapter will focus primarily on processes of gas transport in unsaturated media. The following issues will be evaluated:

1. How does gas move through the unsaturated zone?
2. How does one evaluate single gas and multicomponent gas transport?
3. How does one measure or estimate the various parameters required to quantify gas flow?
4. How does one numerically simulate gas flow?

Although chemical reactions are discussed in another part of this book, the model equations developed in this chapter need to be incorporated into them. The reader may find the discussion of water flow in unsaturated media in Chapters 3 and 4 helpful in understanding many of the concepts in this chapter.

8.1.1 GAS CONTENT

Unsaturated media consist generally of at least three phases: solid, liquid and gas. In some cases, a separate nonaqueous liquid phase may exist if the system is contaminated by organic compounds. In most cases the pore space is only partly filled with gas. The volumetric gas content (θ_G) is defined as:

$$\theta_G = V_G / V_T \tag{8.1}$$

where V_G (L^3) is the volume of the gas and V_T (L^3) is the total volume of the sample. This definition is similar to that used for volumetric water content in unsaturated-zone hydrology. In many cases, the volumetric gas content is referred to as the gas porosity. The saturation with respect to the gas phase (S_G) is:

$$S_G = V_G / V_v \tag{8.2}$$

where V_v (L^3) is the volume of voids or pores. Saturation values range from 0 to 1. Volumetric gas content and gas saturation are related as follows:

$$\theta_G = \phi S_G \tag{8.3}$$

where ϕ is porosity (V_p / V_T). If only two fluids, gas and water, are in the system, the volumetric gas and water contents sum to the porosity. Therefore, volumetric gas content can be calculated if the volumetric water content and porosity are known. Volumetric water content can be measured using procedures described in Gardner (1986).

   In unsaturated systems, water is the wetting and gas is the nonwetting phase. Therefore, water wets the solids and is in direct contact with them, whereas gas is generally separated from the solid phase by the water phase. Water fills the smaller pores, whereas gas is restricted to the larger pores.

8.1.2 Differences between Gas and Water Properties

Gas and water properties differ greatly and can be compared as follows: (1) gas density is much lower than liquid density. The density of air varies with composition but ranges generally from 1 to 1.5 kg m^{-3}, whereas the density of water is close to 1,000 kg m^{-3} (Table 8.1); (2) although water is generally considered incompressible, the incompressibility assumption is not always valid for gas flow. Gas density depends on gas pressure, which results in a nonlinear flow equation; (3) at solid surfaces, water is assumed to have zero velocity whereas gas velocities are generally nonzero, and such velocities result in slip flow or the Klinkenberg effect (Figure 8.1); (4) because the dynamic viscosity of air is ~ 50 times lower than that of water, significant air flow can occur at much smaller pressure gradients. Gas viscosity increases with temperature, whereas water viscosity decreases with temperature; (5) air conductivities are generally an order of magnitude less than water or hydraulic conductivities in the same material because of density and viscosity differences between the fluids; (6) because gas molecular diffusion coefficients are about four orders of magnitude greater than those of water, gas diffusive fluxes are generally much greater than those of water.

8.1.3 Terminology

Gas refers to a phase that may be single or multicomponent. Gas flux can be expressed in a variety of ways, such as volume (L^3 L^{-2} t^{-1}), mass (M L^{-2} t^{-1}), molar (mol L^{-2} t^{-1}) or molecular (number of molecules L^{-2} t^{-1}) fluxes. If a gas is incompressible, (density constant), then volume and mass are conservative, whereas if a gas is compressible only mass is conservative. The mean mass flux is weighted by the mass of each molecule. In the mean molar or molecular flux all molecules behave identically and contribute equally to the mean. The distinction between mass and molar flux will be clarified in Section 8.1.5.4. Parameters important in describing gas transport mechanisms include mean free path (λ), which is the average distance a gas molecule travels before colliding with another gas molecule; pore size (λ_p), which is equivalent to the average distance between soil particles in dry porous media; and particle size (r_p). Equimolar component gases are

TABLE 8.1

Variations in density and viscosity with temperature for water, water vapor, and air. Moist air corresponds to a vapor pressure of 4.6 mm at 0°C to 261 mm at 100°C.

T (°C)	[1]Density water (kg m^{-3})	[2]Density water vapor (kg m^{-3})	[3]Density moist air (kg m^{-3})	[4]Viscosity water (Pa s)	[5]Viscosity water vapor (Pa s)	[6]Viscosity dry air (Pa s)
0	1000	0.005	1.290	1.79E-03	8.03E-06	1.73E-05
10	1000	0.009	1.242	1.31E-03	8.44E-06	1.77E-05
20	998	0.017	1.194	1.00E-03	8.85E-06	1.81E-05
30	996	0.030	1.146	7.97E-04	9.25E-06	1.85E-05
40	992	0.051	1.097	6.53E-04	9.66E-06	1.89E-05
50	988	0.083	1.043	5.48E-04	1.01E-05	1.93E-05
60	983	0.130	0.981	4.70E-04	1.05E-05	1.97E-05
70	978	0.198	0.909	4.10E-04	1.09E-05	2.01E-05
80	971	0.293	0.823	3.62E-04	1.13E-05	2.05E-05
90	965	0.423	0.718	3.24E-04	1.17E-05	2.09E-05
100	959	0.598	0.588	2.93E-04	1.21E-05	2.13E-05

[1,3,4]Weast, 1986; [2]Childs and Malstaff (1982), in Hampton (1989); [5,6]White and Oostrom (1996). Vapor pressure of moist air ranges from 4.6 mm at 0°C to 761 mm at 100°C.
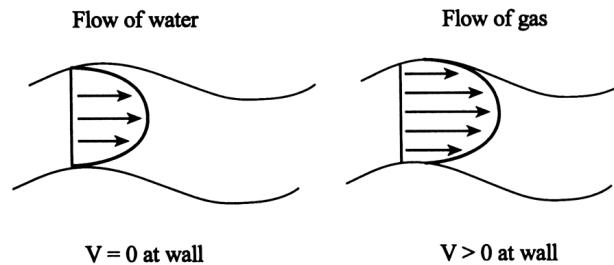
FIGURE 8.1 Schematic demonstrating zero velocities at pore walls of liquid flow and nonzero velocities of gas flow.

components that have the same molecular weight, such as N_2 and CO, whereas nonequimolar component gases have different molecular weights. The terms *concentration* (M L^{-3}) and *partial pressure* (M L^{-1}t^{-2}) refer to individual gas components. The partial pressure of gas component *i* is equal to the mole fraction times the total pressure and can be related to concentration through the ideal gas law for ideal gases. Advective flux refers to bulk gas phase and occurs in response to unbalanced mechanical driving forces acting on the phase as a whole.

8.1.4 MASS TRANSFER VERSUS MASS TRANSPORT

Most of this chapter deals with transport of gas and associated chemicals through the unsaturated zone. Mass transfer refers to transfer of mass or partitioning of mass among gas, liquid and solid phases. Partitioning of chemicals into other phases retards their transport in the gas phase and can be described by:

$$C_T = \rho_b C_{ad} + \theta_l C_l + \theta_G C_G \qquad [8.4]$$

where C_T is the total mass concentration (M L^{-3} soil); C_G, C_l, and C_{ad} are the mass concentrations in the gas and liquid phases and adsorbed on the solid phase; and ρ_b is the bulk density (M L^{-3}). The relationship between gas and water mass concentrations can be described by Henry's law:

$$C_G = K_H C_l \qquad\qquad\qquad [8.5]$$

where K_H is the dimensionless Henry's law constant. Many types of isotherms describe the adsorption onto the solid phase, the simplest being the linear adsorption isotherm:

$$C_{ad} = K_d C_l \qquad\qquad\qquad [8.6]$$

where K_d (L^3 M^{-1}) is the distribution coefficient. The linear relationship generally applies to low polarity compounds (Brusseau, 1994).

If linear relationships are valid, total concentration can be written in terms of gas concentration as follows (Jury et al., 1991):

$$C_T = (\rho_b K_d / K_H + \theta_l / K_H + \theta_G)C_G = B_G C_G \qquad\qquad [8.7]$$

where B_G is the bulk gas phase partition coefficient (Charbeneau and Daniel, 1992). In some studies this partitioning behavior is used to quantify the amount of a liquid phase in the system. For example, transport of gas tracers that partition into water or nonaqueous phase liquids is compared with transport of those that do not partition (conservative) into that phase to determine the amount of water or organic compound in the system (Jin et al., 1995).

8.1.5 MECHANISMS OF GAS TRANSPORT

Many readers may be more familiar with transport mechanisms in the liquid than in the gas phase. Primary mechanisms of solute transport in the liquid phase include advection (movement with the bulk fluid) and hydrodynamic dispersion (mechanical dispersion and molecular diffusion) (Freeze and Cherry, 1979). Mechanical dispersion, resulting from variations in fluid velocity at the pore scale, is the product of dispersivity and advective velocity. Transport in the gas phase may also be described by advection and dispersion. Although some studies have found mechanical dispersion or velocity-dependent dispersion to be important for chemical transport in the gas phase (Rolston et al., 1969; Auer et al., 1996), in most cases mechanical dispersion is ignored because gas velocities are generally too small and the effects of diffusion are generally much greater than dispersion in the gas phase. Molecular diffusion coefficients are approximately four orders of magnitude greater in the gas than in the liquid phase.

Diffusive transport in the liquid phase is described by molecular diffusion. Traditionally, diffusive transport in the gas phase has also been described by molecular diffusion. Diffusion in the gas phase may, however, be much more complicated and may include Knudsen, molecular and nonequimolar diffusion. Surface diffusion of adsorbed gases, generally not significant, is not discussed in this chapter. Pressure diffusion results from the separation of gases of different molecular weights under a pressure gradient and causes diffusion of heavier (lighter) molecules toward regions of higher (lower) pressure (Amali and Ralston, 1993). Pressure diffusion is generally negligible at depths of less than 100 m, which include most unsaturated sections (Amali and Rolston, 1993). Although temperature gradients in unsaturated media are generally too low to result in significant diffusion except at the land surface, thermal diffusion is important for water vapor transport (Section 8.6.3).

8.1.5.1 Advective Flux

If a total pressure gradient exists in a soil as a result of external forces such as atmospheric pumping (Section 8.2), gases will flow from points of higher to those of lower pressure. It has been shown that relatively small gradients in total pressure can result in advective gas fluxes that are much larger than diffusive gas fluxes (Alzaydi and Moore, 1978; Thorstenson and Pollock, 1989; Massmann and Farrier, 1992). The driving force for flow is the total pressure gradient, and the resistance to flow is caused by viscosity of the gas. Other terms for advective flux are pressure driven or viscous flux. Under a total pressure gradient, advection is dominant when the mean free path of the gas molecules (λ) is much less than the pore radius (λ_p) and the particle radius (r_p) ($\lambda \ll \lambda_p$ and $\lambda \ll r_p$), resulting in intermolecular collisions being dominant relative to collisions between gas molecules and the pore walls (Cunningham and Williams, 1980). Because the mean free path is inversely proportional to the mean pressure, low mean free paths relative to pore size may occur in dry, coarse-grained media and/or under high mean pressure. A pressure gradient is required to maintain advective flux because of the velocity reduction near the pore walls caused by gas molecules rebounding from collisions with the pore walls. In unsaturated media the pore walls will generally consist of the gas–liquid interface. Advective flux is also termed nonsegregative or nonseparative because bulk flow as a result of a pressure gradient does not segregate the gas into individual components. The viscous flux of gas component i is proportional to its mole fraction (x_i) in the mixture:

$$N_i^V = x_i N^V \tag{8.8}$$

where N_i^V is the molar viscous flux (mol L^{-2} t^{-1}) of gas i and N^V is the total molar viscous flux. As the mean pressure and/or as the pore size decrease as a result of decreasing grain size or gas saturation (increasing water saturation), a continuum results, from advective or viscous flux to viscous slip flux (Klinkenberg effect) to Knudsen diffusive flux. Viscous slip flux occurs when the mean free path of the gas molecules becomes approximately the same as the pore radius and results from nonzero velocity at the pore wall. Stonestrom and Rubin (1989) and Detty (1992) found that errors resulting from ignoring viscous slip flux in dry, coarse-grained porous media (sands) were less than 7%.

8.1.5.2 Knudsen Diffusive Flux

Knudsen flux occurs when the gas mean free path is much greater than the pore radius ($\lambda \gg \lambda_p$), Knudsen number ($K_n = \lambda/\lambda_p$) = 10 corresponding to the Knudsen regime (Alzaydi, 1975; Abu-El-Sha'r, 1993). Molecule–wall collisions dominate over molecule–molecule collisions. The term *free molecule flux* is also used to describe Knudsen flux because rebounding molecules do not collide with other gas molecules. The Knudsen diffusive flux depends on the molecular weights and temperatures of gases and the radius of the pores. It is not influenced by the presence of other species of gas and is described as follows:

$$N_i^k = -D_i^k \nabla C_i \tag{8.9}$$

where N_i^k is the Knudsen molar flux of component i (mol L^{-2} t^{-1}), D_i^k is the effective Knudsen diffusivity (L^2 t^{-1}), and C_i is the molar concentration of gas i (mol L^{-3}) (Cunningham and Williams, 1980). D_i^k is defined as:

$$D_i^k = Q_p \left(\frac{RT}{M_i} \right)^{0.5} \tag{8.10}$$

where Q_P is the Knudsen radius (L), R is the ideal gas constant (M L^2 t^{-2} T^{-1} mol^{-1}), T is temperature (T), and M_i is the molecular weight of gas i (M mol^{-1}).

8.1.5.3   Molecular Diffusive Flux

Molecular diffusion is the only type of transport mechanism that occurs under isothermal, isobaric conditions when equimolar pairs of gases (e.g., N_2, CO) counterdiffuse in pores whose size is much greater than that of the mean free path of the gas molecules. In this case molecule–molecule collisions dominate over molecule–wall collisions. The molecular diffusive flux depends on gas molecular weights and temperatures in the pore space and is unaffected by the physical nature of the pore walls. Because molecular diffusion results in segregation of the different component gases, it is termed *segregative*. The molar diffusive flux of component i resulting from molecular diffusion J_{iM}^m, in a binary gas mixture under isothermal, isobaric conditions is proportional to the concentration gradient and is described by Mason and Malinauskas (1983):

$$J_{iM}^m = -D_{ij}^e \nabla n_{iM} \qquad [8.11]$$

where D_{ij}^e is the effective molecular diffusion coefficient (L^2 t^{-1}) and n_{iM} is the molar concentration of gas i (mol L^{-3}) (Abu-El-Sha'r, 1993). The effective diffusion coefficient in porous media is calculated from the free air diffusion coefficient as follows:

$$D_{ij}^e = \tau \theta_G D_{ij} \qquad [8.12]$$

where τ is the tortuosity, θ_G is the gas content and D_{ij} is the free air diffusion coefficient (L^2 t^{-1}). Volumetric gas content (θ_G) accounts for reduced cross-sectional area in porous media relative to free air, and tortuosity (τ) accounts for increased path length. A variety of equations have been developed to calculate tortuosity. The most commonly used equations are those of Penman (1940a, b) and Millington and Quirk (1961) (Table 8.2). The effective diffusion coefficient decreases with increased water content in unsaturated systems; the rate of decrease is low at low water contents because gas is in the large and water in the small pore spaces. The effective diffusion coefficient decreases sharply as soils become saturated with water because the large pores become occluded.

8.1.5.4   Bulk Diffusive Flux

Bulk diffusion includes molecular and nonequimolar diffusion. Nonequimolar diffusion occurs when gas components have different molecular weights. According to the kinetic theory of gases, gas molecules have the same kinetic energy in an isothermal, isobaric system; therefore, lighter gas molecules have higher velocities than heavier gas molecules. In a binary mixture of nonequimolar gases, the more rapid diffusion of the lighter gas molecules results in a pressure gradient. Such pressure gradients should be distinguished from external pressure gradients that result in advective flux. The flux resulting from the buildup of pressure is diffusive and is called the *nonequimolar flux* or the *diffusive slip flux* (Cunningham and Williams, 1980). Because the nonequimolar flux does not result in separation of gas components (nonsegregative), the molar bulk diffusive flux includes the segregative molecular diffusive flux and the nonsegregative nonequimolar diffusive flux:

$$N_i^D = J_{iM}^m + x_i \sum_{j=1}^{\nu} N_j^D \qquad [8.13]$$

TABLE 8.2
Models for estimating tortuosity, θ_G is the gas content, and ϕ is the porosity; a more complete listing is provided in Abu-El-Sha'r (1993).

Tortuosity (τ) times θG	Reference	Comments
0.66ϕ	Penman (1940a, b)	experimental
$\left(\theta_G\right)^{3/2}$	Marshall (1958)	pseudotheoretical
$\left(\theta_G\right)^{4/3}$	Millington (1959)	pseudotheoretical
$\theta_G^{-10/3} / \phi^2$	Millington and Quirk (1961)	theoretical
$(1-S_w)^2 * (\phi-\theta)^{2x}$	Millington and Shearer (1970)	theoretical
$\theta_G^{7/3}$	Lai et al. (1976)	experimental
0.435ϕ	Abu-El-Sha'r Abriola (1997)	experimental

where N_i^D is the bulk molar diffusive flux of component i (mol L^{-2} t^{-1}), J_{iM}^m is the molar diffusive flux of component i resulting from molecular diffusion, x_i is the mole fraction of component i, ν is the number of gas components, and the second term on the right $x_i \sum_{j=1}^{\nu} N_j^D$ is the nonequimolar flux.

It is important to distinguish between diffusive gas flux with respect to average velocity of the gas molecules (molar velocity) and that with respect to velocity of the center of mass of the gas (mass velocity) because the two are not necessarily the same (Cunningham and Williams, 1980). In nonequimolar gas mixtures, because the lighter gas molecules diffuse more rapidly, the molar gas flux moves in the direction in which the lighter gas molecules are moving, whereas the center of mass of the gas moves in the direction in which the heavier molecules diffuse. The molar and mass fluxes can therefore move in opposite directions.

8.1.6 GAS TRANSPORT MODELS

Darcy's law is used to model advective or viscous gas transport, and traditionally Fick's law has been used to model molecular diffusion. The Stefan-Maxwell equations and the dusty gas model can also be used to simulate diffusive gas flux. If there is a total pressure gradient in a system, then the diffusive fluxes are calculated relative to the bulk molar flux. The total molar flux is calculated by adding the molar viscous or advective flux to the bulk molar diffusive flux:

$$N_i^T = N_i^V + N_i^D$$

[8.14]

where N_i^T is the total gas molar flux, N_i^V is the molar viscous flux and N_i^D is the molar diffusive flux of component i. For analysis of transient gas flux, the constitutive flux equations are incorporated into the conservation of mass. If the mass density of the fluid and the diffusion coefficients are assumed constant, then the transport equation can be written as:

$$\frac{\partial(Cx_i)}{\partial t} + \nabla \cdot \left(N_i^T\right) = 0$$

[8.15]

where C is the molar concentration of the gas (mol L^{-3}) and x_i is the mole fraction of component i (Massmann and Farrier, 1992). This equation is strictly valid for relatively dilute gas mixtures or for vapors with molecular weights close to the average molecular weight of air (Bird et al., 1960).

8.1.6.1 Darcy's Law

Darcy's law is used to describe advective gas transport. The simplest form of Darcy's law is as follows:

$$J_G = -\frac{k_G}{\mu_G}\nabla P \qquad [8.16]$$

where J_G is the volumetric flux (L^3 L^{-2} t^{-1}), k_G is the permeability (L^2), μ_G is the dynamic gas viscosity (M L^{-1} t^{-1}), and ∇P is the applied pressure gradient. Gravity gradients, assumed negligible here, are treated in Section 8.2.1. The ideal gas law can be used to convert the volumetric gas flux (J_G) to the molar gas flux (N^V):

$$PV = nRT, \qquad \rho_G = \frac{nM}{V} = \frac{PM}{RT} \qquad [8.17]$$

where n is the number of moles of the gas, M is the molar mass of the gas, R is the ideal gas constant (M L^2 t^{-2} T^{-1} mol^{-1}) and T is temperature (K). The molar viscous or advective flux is:

$$N^V = -\frac{P}{RT}\frac{k_G}{\mu_G}\nabla P \qquad [8.18]$$

The validity of Darcy's law can be evaluated by plotting the gas flux for a single component against the pressure gradient. The relationship should be linear with a zero intercept if Darcy's law is valid.

8.1.6.2 Fick's Law

Fick's law is an empirical expression originally developed to describe molecular diffusion of solutes in the liquid phase. Fick's law is generally used to describe molecular diffusion of gas i in gas j (Bird et al., 1960; Jaynes and Rogowski, 1983):

$$J_{iM}^m = -D_{ij}C\nabla x_i \qquad [8.19]$$

where C is the total molar concentration (mol L^{-3}, constant in an isothermal, isobaric system) and x_i is the mole fraction of gas and $D_{ij} = D_{ji}$ (Bird et al., 1960). Fick's law is strictly applicable to molecular diffusion of equimolar gases in isothermal, isobaric systems. Fick's law excludes the effects of Knudsen diffusion and nonequimolar diffusion. Fick's law can predict the flux of only one component. The adequacy of Fick's law will be discussed after the other models have been described.

8.1.6.3 Dusty Gas Model

In contrast to Fick's law, which is empirical, the dusty gas model is based on the full Chapman Enskog kinetic theory of gases. Application of the kinetic theory of gases is only possible by considering the dust particles (porous medium) as giant molecules that constitute another component in the gas phase. The multicomponent equations, which are based on the dusty gas model originally proposed by Mason et al. (1967), are presented by Satterfield and Cadle (1968), Cunningham and

Williams (1980), Mason and Malinauskas (1983), and Thorstenson and Pollock (1989). The equations for the dusty gas model of binary and multicomponent gas diffusion are (Cunningham and Williams, 1980):

$$\frac{x_1 N_2^D - x_2 N_1^D}{D_{12}^e} \; - \; \frac{N_1^D}{D_1^k} \; = \; \frac{\nabla P_1}{RT}$$

$$\sum_{\substack{i=1 \\ i \neq j}}^{v} \frac{x_i N_j^D - x_j N_i^D}{D_{ij}^e} \; - \; \frac{N_i^D}{D_i^k} \; = \; \frac{\nabla P_i}{RT} \qquad [8.20]$$

$$\underset{\substack{\text{molecular} \\ \text{diffusion}}}{} \quad \underset{\substack{\text{Knudsen} \\ \text{diffusion}}}{} \quad \underset{\substack{P\,\text{gradient} \\ \text{term}}}{}$$

where x_i is the mole fraction of component i, N_i^D is the bulk molar diffusive flux of gas component i (mol L^{-2} t^{-1}), D_{ij}^e is the effective molecular diffusivity (L^2 t^{-1}), D_i^k is the effective Knudsen diffusivity (L^2 t^{-1}), and P_i is the partial pressure of component i (M $L^{-1}t^{-2}$). Although one generally writes equations in terms of a flux of a component being proportional to a gradient, multicomponent gas equations are simplest when written in terms of a gradient of gas component i being proportional to the fluxes of all other components (Mason and Malinauskas, 1983). Derivation of the above form of these equations for a binary gas mixture is shown in Section 8.7. Knudsen diffusion is important when the second term in the dusty gas model is larger than the first term. This requires that $D_i^k \ll D_{ij}^e$ which appears counterintuitive (Thorstenson and Pollock, 1989), but which can be understood if one considers the reciprocal of D_i^k as a resistance. Knudsen diffusion is thus important when $1/D_i^k$ is large and D_i^k is small. Although there is a gradient in the natural log of temperature in the dusty gas model (Thorstenson and Pollock, 1989), gradients in temperature in the subsurface are generally small and gradients in the natural log of temperature are generally negligible. It has therefore been omitted in Equation [8.20]. The primary assumptions of the dusty gas model are that the dust particles are spherical and that there are no external forces on the gas. The dusty gas model can predict the flux of all components in a gas mixture. The system of equations can be solved analytically (Jackson, 1977) or numerically (Massmann and Farrier, 1992). Many analyses of the dusty gas model assume steady-state flow (Thorstenson and Pollock, 1989; Abu-El-Sha'r, 1993).

When both partial and total pressure gradients are important for gas flux, the combined effects of advection and diffusion need to be considered. Knudsen diffusion, which is proportional to the total mole fraction, provides the link between advection and diffusion. Because the dusty gas model is the only model that includes Knudsen diffusion, it is the only model that can theoretically link advection and diffusion through the Knudsen diffusion term. The dusty gas model for combined advection and diffusion is as follows (Thorstenson and Pollock, 1989):

$$\sum_{\substack{j \neq 1 \\ j \neq i}}^{v} \frac{x_i N_j^T - x_j N_i^T}{D_{ij}^e} - \frac{N_i^T}{D_i^k} = \frac{P \nabla x_i}{RT} + \left(1 + \frac{kP}{D_i^k \mu_G}\right) \frac{x_i \nabla P}{RT} \qquad [8.21]$$

where x_i is the mole fraction of component i, N_i^T is the total molar gas flux of component i relative to a fixed coordinate system (mol L^{-2}, t^{-1}), D_{ij}^e is the effective molecular diffusion coefficient of component i in j (L^2 t^{-1}), D_{ij}^K is the effective Knudsen diffusion coefficient of component i (L^2 t^{-1}), P is pressure (M L^{-1} t^{-2}), R is the ideal gas constant, T is absolute temperature, k is permeability (L^2) and μ_G is gas viscosity (M L^{-1} t^{-1}).

8.1.6.4 Stefan-Maxwell Equation

The Stefan-Maxwell equations, which can predict the fluxes of all but one gas component in a multicomponent gas mixture, can be obtained from the dusty gas model by assuming negligible Knudsen diffusion (no molecule particle collisions):

$$\sum_{\substack{j=1 \\ j \neq i}}^{v} \frac{x_i N_j^D - x_j N_i^D}{D_{ij}^e} \quad = \quad \frac{\nabla P_i}{RT} \qquad [8.22]$$

8.2 TRANSPORT OF A HOMOGENEOUS GAS

Transport of a homogeneous gas in dry, coarse-grained media can be described by advection. Because such a gas can be considered as a single component, the only type of diffusion possible is Knudsen diffusion. Single-component gases in dry, coarse-grained media are dominated by advective or viscous flux because Knudsen diffusion is negligible in such systems. This analysis of gas transport is appropriate when gas velocities are high. The single fluid, nonreactive, noncompositional approximation is appropriate only when one is interested in the bulk flow of a homogeneous gas.

Natural advective gas transport can occur in response to barometric pressure fluctuations, wind effects, water-table fluctuations, density effects, and can also be induced by injection or extraction, as in soil vapor extraction systems. Barometric pressure fluctuations consist of (1) diurnal fluctuations due to thermal and gravitational effects, which are on the order of a few millibars, and (2) longer term fluctuations that result from regional scale weather patterns, which are on the order of tens of millibars within a few hours of when a high or low pressure front moves through. The penetration depth of barometric pressure fluctuations increases with the thickness of the unsaturated zone and with the permeability of the medium. Because highs are balanced by lows, the net transport of the gas may be negligible, except in fractured media, where contaminants may migrate large distances (Nilson et al., 1991). Smaller scale fluctuations, such as gusts and lulls related to wind, may be important in fractured media (Weeks, 1993). Water-table fluctuations, resulting in changes in the gas volume, can produce advective flow; however, advective fluxes as a result of water-table fluctuations are considered important only if the rate of rise or decline of the water-table is rapid, the permeability of the material is high and the water table is shallow.

8.2.1 GOVERNING EQUATIONS

Darcy's law, which was developed for water flow in saturated media, can also be applied to single-phase gas flow. Darcy's law is an empirical expression and the general form is:

$$J_G = -\frac{k_G}{\mu_G}\left(\nabla P + \rho_G g \nabla z\right) \qquad [8.23]$$

where J_G is the volumetric flux density ($L^3 L^{-2} t^{-1}$), k_G is gas permeability (L^2), ρ_G is gas density ($M L^{-3}$), g is gravitational acceleration ($L t^{-2}$), μ_G is gas viscosity ($M L^{-1} t^{-1}$), P is pressure ($M L^{-1} t^{-2}$), and z is elevation (L). The negative sign in Equation [8.23] is required because flow occurs in the direction of decreasing pressure. The first term in parentheses is the driving force due to pressure and the second term is the driving force due to gravity. Generally gas density is a function of pressure and composition, and the above form of Darcy's law is the only valid form in these cases. The pressure gradient provides the main driving force for advective gas transport, and the resistance to flow results from the gas viscosity. Small pressure gradients can result in substantial advective

gas fluxes because the resistance to flow is small. The small flow resistance is attributed to the negligible viscosities of gases relative to those of liquids and to the gas being present in the largest pores. If the components of a gas all have the same molecular mass, then gas density is independent of composition and is only a function of pressure.

Under static equilibrium and isothermal conditions, gas does not move. If the only forces operating on the gas are pressure and gravity, then these two forces must be balanced. The condition of zero motion results when:

$$\nabla P = -\rho_G g \nabla z \qquad [8.24a]$$

$$\frac{dP}{dz} = -\rho_G g \qquad [8.24b]$$

If gas density varies because of variable composition, the above equation cannot be simplified further. If the gas is barotropic (i.e., $\rho_G = \rho_G(P)$ only), however, the ideal gas law (Equation [8.17]) can be used to relate density and pressure when pressure variations are close to atmospheric. Equation [8.24a] can be solved through integration by inserting the ideal gas law:

$$\frac{RT}{gM} \int_{P_0}^{P} \frac{dP}{P} = -\int_{z_0}^{z} dz; \quad \frac{RT}{gM} \ln\left(\frac{P}{P_0}\right) = -z$$

$$P = P_0 \exp\left(-\frac{Mg}{RT} z\right) \qquad [8.25]$$

where P is assumed to be equal to P_0 at $z = 0$. If $z = 1$ m, $T = 290$ K, R is 8.314 J mol^{-1} K^{-1}, M is 28.96 g mol^{-1} (air), and g is 9.8 m s^{-2}, then $P = 0.99988\ P_0$. Gas pressure therefore changes by 0.012% over a height of 1 m. Because the gas pressure changes are so small, pressure can generally be considered independent of height.

If gas density is only a function of pressure, (compressible gas), Equation [8.23] can be manipulated to obtain:

$$q_G = -\frac{k_G \rho_G}{\mu_G}\left(\frac{\nabla P}{\rho_G} + g\nabla z\right) = -\frac{k_G \rho_G}{\mu_G}\left(\nabla \int_{P_0}^{P} \frac{dP}{\rho_G} + g\nabla z\right) \qquad [8.26]$$

If gas density is independent of pressure, then the gas is incompressible:

$$\nabla \int_{P_0}^{P} \frac{dP}{\rho_G} = \nabla\left(\frac{P}{\rho_G}\right) \qquad [8.27]$$

$$q_G = -\frac{k_G \rho_G g}{\mu_G}\left(\nabla\left(\frac{P}{\rho_G g}\right) + \nabla z\right) = -\frac{k_G \rho_G g}{\mu_G}(\nabla h + \nabla z) = -\frac{k_G \rho_G g}{\mu_G}(\nabla H) \qquad [8.28]$$

where h is pressure head (L) and H is total head (L, pressure + gravitational head). Because gas densities are generally very low (density of air is approximately three orders of magnitude less

than water density), the gravitational term in Equation [8.23] ($\rho_G g \nabla z$) is generally < 1% of the pressure term and is ignored in most cases, as shown in Equation [8.16]. For transient gas flow, Darcy's law (ignoring gravity, Equation [8.16]), substituted into the conservation of mass equation, results in:

$$\frac{\partial(\rho_G \theta_G)}{\partial t} = -\nabla \cdot \left(-\frac{\rho_G k_G}{\mu_G} \nabla P \right) \tag{8.29}$$

Equation [8.29] is nonlinear because gas density depends on gas pressure and can be linearized in terms of P^2 by assuming ideal gas behavior (Equation [8.17]), which results in (Section 8.7):

$$\frac{\partial P^2}{\partial t} \approx \frac{k_G P_0}{\phi \mu_G} \nabla^2 P^2 \approx \alpha \nabla^2 P^2 \tag{8.30}$$

where $k_G P_0 / \phi \mu_G$ is the pneumatic diffusivity (α). If pressure variations are small, another linear approximation to Equation [8.29] can be obtained:

$$\frac{\partial P}{\partial t} = \frac{k_G P_0}{\phi \mu_G} \nabla^2 P \tag{8.31}$$

Derivations of Equations [8.30] and [8.31] are given in Section 8.7.

8.2.2 GAS PERMEABILITY

Gas permeability describes the ability of the unsaturated zone to conduct gas. Permeability (k) should be simply a function of the porous medium if the fluid does not react with the solid. Gas permeability (k_G; L^2) is related to gas conductivity (K_G) as follows:

$$K_G = k_G \frac{\rho_G g}{\mu_G} \tag{8.32}$$

Some groups use the term *gas permeability* for K_G, which is called *gas conductivity*, and use the term *intrinsic permeability* for k_G, which is called *gas permeability*. Equation [8.32] shows that gas conductivity increases with gas density and decreases with gas viscosity.

The above material describes single-phase gas flow. In unsaturated media, the pore space generally contains at least two fluids, gas and liquid. Darcy's law is applied to each fluid in the system, which assumes that there is no interaction between the fluids (Dullien, 1979). Because the cross-sectional area available for flow of each fluid is less than if the system were saturated with a single fluid, the permeability with respect to that fluid is also less. The gas permeability decreases as the gas saturation decreases. The relative permeability (k_{rG}) is a function of the gas saturation (S_G) and is defined as the permeability of the unsaturated medium at a particular gas saturation ($k_G(S_G)$) divided by the permeability at 100% saturation (k_G):

$$k_{rG}(S_G) = k_G(S_G) / k_G \tag{8.33}$$

Relative permeability varies with (1) fluid saturation, (2) whether the fluid is wetting or nonwetting, and (3) whether the system is wetting or drying (hysteresis).
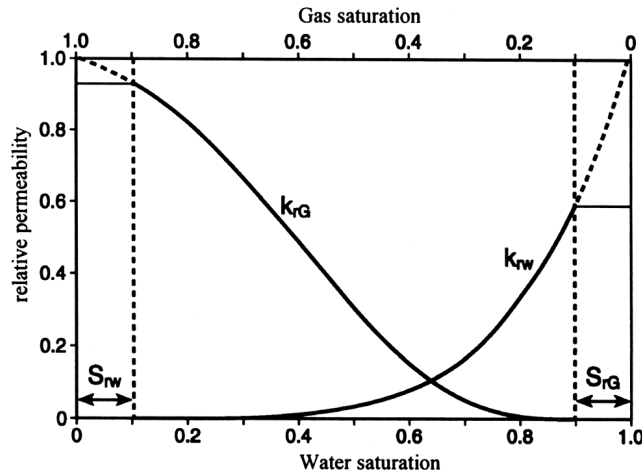
FIGURE 8.2 Schematic relative permeabilities with respect to gas and water saturation.

The relative permeability of the gas phase is greater than that of the liquid phase at low to moderate liquid saturations because the gas generally occurs in larger pores (Demond and Roberts, 1987). Relative permeabilities do not sum to one. This has been attributed to flow pathways traversed by two fluid phases being more tortuous than those traversed by a single phase (Scheidegger, 1974) or to pores with static menisci that cannot result in flow (Demond and Roberts, 1987). Zero relative permeabilities correspond to nonzero fluid saturations (Figure 8.2). For example, in systems initially water saturated that begin to drain, gas will not begin to flow until a minimum gas saturation has been reached, the residual gas saturation (S_{rG}; Figure 8.2). The gas zero relative permeability region corresponds to trapped gas and disruption of gas connectivity caused by water blockages (Stonestrom and Rubin, 1989). Liquid-phase permeability also exhibits a zero-permeability region that corresponds to residual liquid or water saturation (Chapter 3). In natural systems, the zone of residual water saturation corresponds to a zone of constant gas relative permeability because gas content does not increase. The dashed line in Figure 8.2 in this zone corresponds with further increases in gas relative permeability (k_{rG}), which is related to increased gas content if the soil is oven dried and the water content is reduced to zero. A similar effect occurs with the water relative permeability (k_{rw}), where the dashed line shows increased water relative permeability corresponding to vacuum saturation or saturation of the sample under back pressure. Gas permeability is hysteretic at low water content, which indicates that gas permeability is not a unique function of gas saturation but depends on saturation history (i.e., whether the system is drying or wetting). At a given saturation, gas permeability is generally greater for wetting than for drying (Stonestrom and Rubin, 1989).

Various expressions have been developed to relate relative permeability to gas saturation (Table 8.3). Many of the expressions were developed to estimate relative permeabilities with respect to water; the corresponding expressions for gas relative permeability were obtained by replacing the effective liquid saturation (S_e) by $1-S_e$, where S_e is:

$$S_e = \frac{S - S_r}{1 - S_r}$$ [8.34]

where S_r is the residual water saturation (Brooks and Corey, 1964).

Darcy's law can be written as:

$$J_G = -\frac{k_{rG}(S_G)k_G}{\mu_G}(\nabla P) = -\frac{k_G(S_G)}{\mu_G}\nabla P$$ [8.35]

TABLE 8.3
Expressions relating relative gas permeability and saturation. S_e is the effective saturation with respect to water; $S_e = (S_w - S_{rw})/(1 - S_{rw})$, S_{rw} is the residual wetting phase saturation (water in water-air system), λ is the bubbling pressure, and m and n are fitting parameters.

Brooks and Corey (1964)	$k_{rG} = \left(1 - S_e\right)^2 \left(1 - S_e^{\frac{2+\lambda}{\lambda}}\right)$	
Corey (1954)	$k_{rG} = (1 - S_e)^2 (1 - S_e^2)$	
Falta et al. (1989)	$k_{rG} = (1 - S_e)^3$	
van Genuchten (1980); Mualem (1976)	$k_{rG} = \left(1 - S_e^{0.5}\right)\left\{1 - \left[1 - \left(1 - S_e\right)^{1/m}\right]^m\right\}^2$	$m = 1 - 2/n$ $0 < m < 1$
van Genuchten (1980); Burdine (1953)	$k_{rG} = \left(1 - S_e\right)^2 \left\{1 - \left[1 - \left(1 - S_e\right)^{1/m}\right]^m\right\}$	$m = 1 - 2/n$ $0 < m < 1; \ n > 2$

The velocity of the gas particles (V_G) (L t^{-1}) can be calculated from the volumetric flux density by dividing by the volumetric gas content:

$$V_G = J_G / \theta_G \tag{8.36}$$

8.2.3 DEVIATIONS FROM DARCY'S LAW

Non-Darcian effects such as viscous slip flow and inertial flow can occur under many circumstances. As mentioned earlier, gas flow differs from liquid flow in that the velocity of the gas molecules is nonzero at the pore walls (Figure 8.1) and is called *slip velocity* (Dullien, 1979). Slip flow, or the Klinkenberg effect, results in underestimation of gas flux by Darcy's law. Because of slip flow, permeability depends on pressure and the flow equation is nonlinear (Collins, 1961). Klinkenberg (1941) evaluated the relationship between slip-enhanced, or apparent, permeability k_G (L^2) and the permeability at infinite pressure k (L^2) when the gas behaves like a liquid:

$$k_G = k\left[1 + \frac{4c\lambda}{\bar{\lambda}_p}\right] \tag{8.37}$$

where c is a constant characteristic of the porous medium, λ is the mean free path of the gas at the mean pressure, and $\bar{\lambda}_p$ is the mean pore radius (Klinkenberg, 1941). Because the mean free path is inversely proportional to the mean pressure in the system, the equation can be modified to:

$$k_G = k\left(1 + \frac{b_i}{\bar{P}}\right) \tag{8.38}$$

where $\bar{P}$ is the mean pressure and b_i (M L^{-1} t^{-2}) is a constant (slip parameter) that depends on the porous medium and the gas i used in the measurement (Klinkenberg, 1941). These two equations show that gas slippage, or slip-enhanced permeability, is enhanced when the mean pressure is low. As the mean pressure increases, gas permeability decreases and approaches liquid permeability.

Detty (1992) found that the slip parameter is not only a function of the reciprocal mean pressure as indicated by Klinkenberg (1941), but also a function of the pressure gradient and saturation. Slip correction factors measured in unconsolidated sands are generally fairly low (1 to 6%) (Stonestrom and Rubin, 1989; Detty, 1992) and resemble those measured in consolidated sands (Estes and Fulton, 1956).

Non-Darcian behavior can also occur at high flow velocities as a result of inertial effects. According to Darcy's law, the flux is linearly proportional to the pressure gradient. At high flow velocities, the relationship becomes nonlinear and inertial effects result in fluxes lower than those predicted by Darcy's law. Forcheimer (1901) modified Darcy's law for high velocities:

$$\nabla P = \frac{\mu_G J_G}{k_G} + \beta \rho_G J_G{}^2 \qquad\qquad [8.39]$$

where P is pressure, μ_G is gas viscosity, J_G is volumetric gas flux, and β is the inertial flow factor (L^{-1}) (Detty, 1992). The second-order term results from kinetic energy losses from high-velocity flows. There is a spectrum from viscous (linear–laminar or Darcy flow) to inertial flow (fully turbulent) with a visco-inertial regime in between. Laminar flow is not restricted to the region where Darcy's law is valid, but extends into the visco-inertial regime where nonlinear–laminar flow occurs ($q \sim \nabla P^n$) (Detty, 1992). Detty (1992) indicated that deviations from viscous flow can be significant. The flow rates and pressure gradients that result in visco-inertial flow vary with water saturation.

8.3 MULTICOMPONENT GAS TRANSPORT

In isobaric systems, gas transport occurs by diffusion, whereas in nonisobaric systems gas transport occurs by advection (Darcy's law) and diffusion. A variety of models are available to describe multicomponent gas diffusion. Traditionally, gas diffusion has been described by Fick's law. As noted earlier, Fick's law is valid strictly for isothermal, isobaric and equimolar countercurrent diffusion of a binary gas mixture. Theoretical analysis by Jaynes and Rogowski (1983) shows that the diffusion coefficient of Fick's law is only a function of the porous medium under certain conditions: equimolar countercurrent diffusion in a binary gas mixture, diffusion of a dilute component gas in a multicomponent gas mixture, and diffusion in a ternary system when one gas component is stagnant (zero flux, no sources or sinks, no reactions). Studies by Leffelaar (1987) indicate that if binary gas diffusion coefficients differ by more than a factor of 2, then Fick's law is invalid. Amali and Rolston (1993) also added that the total mole fraction of the diffusing gas components needs to be considered and should be low in order for Fick's law to be applicable.

If the flux of each gas component depends on the flux of the other gas components, then Fick's law no longer applies. In some cases, the calculated Fick's law flux is not only different in magnitude relative to multicomponent molecular diffusive flux, but opposite in direction also, as a result of molecular diffusion against a concentration gradient (Thorstenson and Pollock, 1989). Because Fick's law predicts the diffusion of only one component, variations in concentration of other components are attributed to other processes. Baehr and Bruell (1990) showed that physical displacement of naturally occurring gases such as O_2 by organic vapors and evaporative advective fluxes can be incorrectly attributed to aerobic microbial degradation or other sink terms when Fick's law is used. Unlike Fick's law, which can only consider binary gas mixtures, the Stefan-Maxwell equations or the dusty gas model can evaluate multicomponent gas transport. For multicomponent analysis, the transport of one component depends upon the transport of all other components that are present in the gas mixture. It is impossible to separate fully the effects of diffusion from those of advection in multicomponent gas systems (Thorstenson and Pollock, 1989). As noted earlier, Stefan-Maxwell equations are valid strictly for isobaric systems where Knudsen diffusion is negligible.
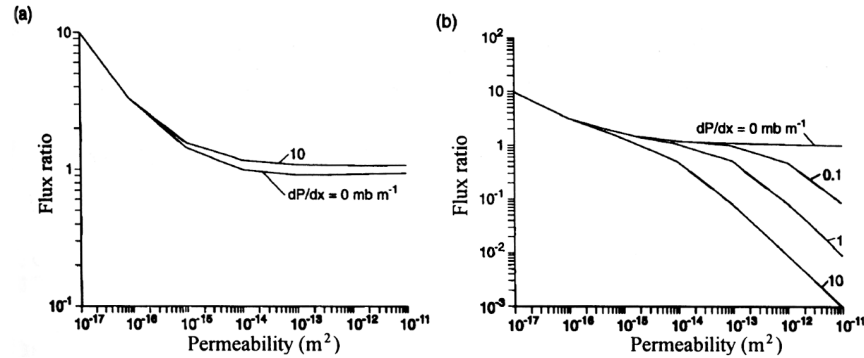
FIGURE 8.3 (a) Ratios of TCE fluxes calculated using the single-component equation (Fick's law for diffusion) divided by fluxes calculated using the dusty gas model; (b) ratios of TCE fluxes calculated using the Stefan-Maxwell equation divided by fluxes calculated using the dusty gas model (Massmann and Farrier, 1992).

The validity of the single-component advection–diffusion (Fick's law) equation for simulating gas phase transport depends on the pore sizes and permeability of the porous media, the relative concentrations of the gas components that are involved, and their molecular weights, viscosities and pressure gradients. Massmann and Farrier (1992) compared fluxes using the single-component advection–diffusion equation with those calculated using the multicomponent Stefan-Maxwell equation and dusty gas model. The comparisons were developed for transport conditions similar to what might be observed in volatile organic compounds (VOCs) in the near surface vadose zone. For total pressure gradients ranging from 100 to 1,000 Pa m^{-1} (1 to 10 mbar m^{-1}), the single-component advection–diffusion (Fick's law) equation significantly overestimates fluxes for toluene and trichloroethylene (TCE) in soils having permeabilities on the order of 10^{-16} to 10^{-17} m^2 (Figure 8.3a). These permeabilities might correspond to unweathered clays, glacial tills or very fine silts (Table 8.4). The Stefan-Maxwell equations also overestimate fluxes in this permeability range because Knudsen diffusion is not included in Fick's law or in the Stefan-Maxwell equations (Figure 8.3b). The flux predicted by the single-component advection–diffusion equation is within a factor of 2 of that predicted by the dusty gas model in materials having permeabilities greater than 10^{-14} m^2. This permeability corresponds to a relatively dry silty-sand material (Table 8.4). The Stefan-Maxwell equation underestimates fluxes in high-permeability materials for moderate total pressure gradients (0.1 to 1 mbar m^{-1}; 10 to 100 Pa m^{-1}) (Figure 8.3b). Massmann and Farrier (1992) also illustrated how multicomponent equations may result in situations in which diffusion can occur in a direction opposite that of the partial-pressure gradients. In multicomponent equations, the diffusive flux of one component depends on the diffusive fluxes of all other components in the system. For example, a large partial-pressure gradient for TCE can cause the diffusive flux of N_2 and O_2 to occur in a direction opposite to their partial pressure gradients. In general, single component equations will be more valid for dilute gases having molecular weights similar to those of other species in the gas mixture.

Abriola et al. (1992) evaluated advective and diffusive fluxes in a system comprising two components. They reported that under an applied total pressure gradient of 0.05 mbar m^{-1} (5 Pa m^{-1}), the single and multicomponent models give virtually indistinguishable results for transport predictions in a sandy soil. For transport in a low permeability material, such as a clay under a total pressure gradient of 0.05 mbar m^{-1}, diffusive fluxes dominate, and single- and multicomponent equations give different transport predictions. Multicomponent gas experiments that evaluated transport of methane and TCE in air were examined by Abu-El-Sha'r (1993). The system was evaluated as either a binary (considering N_2 and O_2 in air as a single component with methane or TCE as the other component) or a ternary system. Results of the experiments showed that model predictions based on Fick's law, the Stefan-Maxwell equations and the dusty gas model were

TABLE 8.4

Typical values of permeability for different types of sediments and rocks.

(From Terzaghi and Peck, 1968, John Wiley & Sons, New York.)

| 10^{-7} | 10^{-8} | 10^{-9} | 10^{-10} | 10^{-11} | 10^{-12} | 10^{-13} | 10^{-14} | 10^{-15} | 10^{-16} | 10^{-17} | 10^{-18} | 10^{-19} | 10^{-20} | m^2 |

| Clean gravel | Clean sands, clean sand and gravel mixtures | Very fine sands, silts, mixtures of sand, silt, and clay, stratified clay deposits, etc. | Homogeneous clays below zone of weathering |
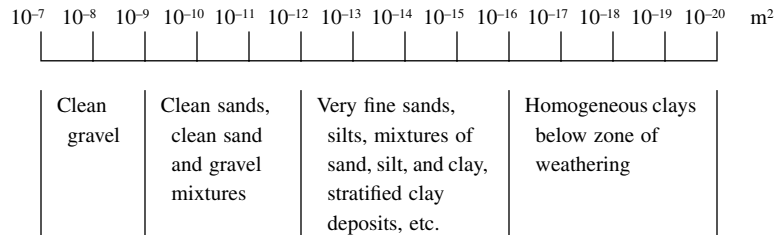
(From Freeze and Cherry, 1979, *Groundwater*, 604, Table 2.2, p. 29, Prentice-Hall, Englewood Cliffs, NJ.)

| 10^{-7} | 10^{-8} | 10^{-9} | 10^{-10} | 10^{-11} | 10^{-12} | 10^{-13} | 10^{-14} | 10^{-15} | 10^{-16} | 10^{-17} | 10^{-18} | 10^{-19} | 10^{-20} | m^2 |

Gravel

Clean sand and silty sand

Silt, loess

Glacial till

Unweathered marine clay

Shale
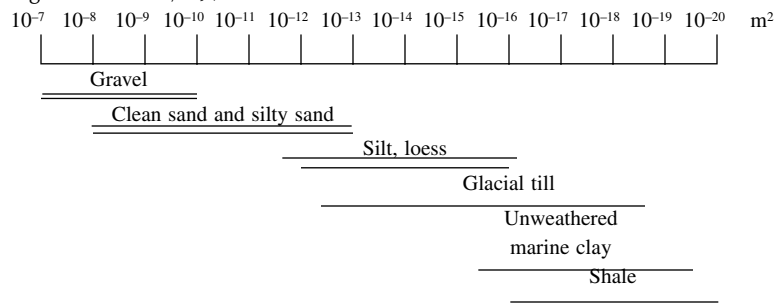
indistinguishable in sand samples, whereas the dusty gas model provided slightly better predictions in kaolinite. All three models can therefore predict diffusional gas fluxes under isobaric conditions when transport is dominated by molecular diffusion. However, under pressure gradients, deviations of measured and predicted values of gas fluxes increased with increasing total pressure gradients. All three models underestimated gas fluxes under nonisobaric conditions. Deviations from measured fluxes were lowest for the dusty gas model, increased for the Stefan-Maxwell equations, and were greatest for Fick's law. Theoretical analysis by Thorstenson and Pollock (1989) indicates that multicomponent analysis using the dusty gas model is required for evaluation of stagnant gases such as N_2 or Ar in the air. Analysis of transient gas flux on the basis of column experiments using benzene and TCE shows that Fick's law and the Stefan-Maxwell equations give similar results in the transient phase of the experiment, but that Fick's law underestimates measured fluxes by as much as 10% in the steady-state phase. The Stefan-Maxwell equations gave much better results (Amali et al., 1996).

These studies were used to develop Table 8.5, which generally outlines which models are most applicable under which pressure, permeability and concentration conditions. For low-permeability material, the dusty gas model is required because it incorporates Knudsen diffusion. For high-permeability material under isobaric conditions, Fick's law can be used if the diffusing gas component has a low concentration, whereas the Stefan-Maxwell equation is required if concentration is high because of the interdependence of flux. The Stefan-Maxwell equations or the dusty gas model can be used when Fick's law applies. Similarly, the dusty gas model can also be used when the Stefan-Maxwell equations are valid. Under nonisobaric conditions, Darcy's law is combined with a diffusion model. The single-component advection diffusion (Fick's law) model can be used in low concentration situations in high-permeability material, whereas the dusty gas model is required in high concentration situations. The Stefan-Maxwell equations generally do not apply

TABLE 8.5
Most appropriate model for describing gas flux under different pressure, permeability and concentration conditions. Pressure gradient refers to the existence of an external pressure gradient, concentration refers to concentration of the diffusing gas component, dusty gas model* includes Darcy's law to describe advective gas flow.

Pressure Gradient	Permeability	Low Concentration	High Concentration
Isobaric	low	dusty gas model	dusty gas model
Isobaric	high	Fick's law	Stefan-Maxwell
Nonisobaric	low	dusty gas model*	dusty gas model*
Nonisobaric	high	advection diffusion	dusty gas model

under nonisobaric conditions (Massmann and Farrier, 1992; pressure gradients > 10 Pa m^{-1}, Figure 8.3b).

8.3.1 DENSITY-DRIVEN ADVECTION

Density-driven advective transport, a specific type of multicomponent gas transport, is important for high molecular-weight compounds that have high vapor densities, such as dense volatile organic contaminants (Falta et al., 1989; Mendoza and Frind, 1990; Mendoza and McAlary, 1990). Important factors controlling density-driven advective flow include saturated vapor density, molecular mass of the chemical, and gas phase permeability. Vapor densities are maximized when the air mixture is saturated by the vapor phase of the chemical. Such high saturations are restricted to areas close to the free phase. Numerical simulations indicate that density-driven advective flow in homogeneous media is important at the high permeabilities (> 10^{-11} m^2) typical of sands and gravels (Falta et al., 1989). The presence of fractures can greatly enhance density-driven advective flow.

An order of magnitude estimate of the advective gas flux resulting from density variations may be obtained from (Falta et al., 1989):

$$J_G = -\frac{k_G g}{\mu_G} \nabla(\rho - \rho_0)$$

[8.40]

Equation [8.40] describes steady-state downward flux of fluid of density ρ through a stagnant fluid of density ρ_0 in material of permeability k_G and ignores diffusion and phase partitioning. An estimate of the density potential of the gas mixture (ρ) with respect to air (ρ_0) can be obtained from relative vapor density (ρ_{rv}) (Mendoza and Frind, 1990):

$$\rho_{rv} = \frac{\rho}{\rho_0} \frac{x_c M_c + (1 - x_c)M_a}{M_a}$$

[8.41]

where x_c is the fractional molar concentration of the compound and M_c and M_a are the molecular weights of the compound and air, respectively. Relative vapor density of the source depends on the vapor pressure and molecular weight of the compound (Mendoza and Frind, 1990). Density-driven advection occurs generally in areas contaminated by high-molecular-weight volatile organic contaminants that have high vapor densities.

8.4 METHODS

8.4.1 ESTIMATED PARAMETERS

Because theoretically permeability should be independent of fluid used, gas and liquid permeabilities should be the same. In fine-grained media or under small mean pressures, gas permeability is greater than liquid permeability because of gas slippage (Klinkenberg effect). Permeability can be corrected for gas slippage using Equation [8.38]. If gas slippage is negligible, as in coarse media having high mean pressures, gas conductivity can be estimated from hydraulic conductivity by:

$$K_G = K_w \left(\frac{\rho_G}{\rho_w} \right) \left(\frac{\mu_w}{\mu_G} \right) \qquad [8.42]$$

Air conductivities are about one-tenth of hydraulic conductivities because the air density is approximately three orders of magnitude less than water density and air viscosity is approximately 50 times less than water viscosity (Table 8.1). The estimated gas conductivities (Equation [8.42]) assume that pores are completely filled with gas. Typical values of permeability for different sediment textures are found in Freeze and Cherry (1979) and Terzaghi and Peck (1968) (Table 8.4), and permeability varies over 13 orders of magnitude from clay to gravel.

A rough estimate of gas permeability in gas saturated systems can be obtained from particle size data:

$$k = C \left(D_{10} \right)^2 \qquad \text{(Hazen, 1911)} \qquad [8.43]$$

$$k = 1,250 (D_{15})^2 \qquad \text{(Massmann, 1989)} \qquad [8.44]$$

where C is a dimensionless shape factor and D_{10} and D_{15} correspond to the grain diameters at which 10 or 15% of the particles by weight are finer. Other estimates of exponents include 1.65 and 1.85 instead of 2 in the Hazen formula (Shepherd, 1989).

The Klinkenberg b parameter can be estimated according to the following empirical equation developed by Heid et al. (1950) for air-dry consolidated media (standard correction for the Klinkenberg effect by the American Petroleum Industry):

$$b_{air} = \left(3.98 \times 10^{-5} \right) k_\infty^{-0.39} \qquad [8.45]$$

where b is in atmospheres and k_∞ is in cm^2. The Klinkenberg b parameter for any gas (b_i) can be estimated from that for air (b_{air}), developed by Heid et al. (1950) according to the following (Thorstenson and Pollock, 1989):

$$b_i = \left(\mu_i / \mu_{air} \right) \left(M_{air} / M_i \right)^{1/2} b_{air} \qquad [8.46]$$

The Knudsen diffusion coefficient is related to the Klinkenberg effect because both are related to the ratio of the mean free path of the gas molecules to the pore radius. Thorstenson and Pollock (1989) showed how the Knudsen diffusion coefficient (D_i^k) can be estimated from the true permeability and the Klinkenberg b parameter for gas i:

$$D_i^k = k b_i / \mu_i \qquad [8.47]$$

Gas conductivities and permeabilities vary with gas content. Estimates of gas conductivity at different gas saturations are provided by equations listed in Table 8.3.

8.4.2 LABORATORY TECHNIQUES

A variety of laboratory techniques are available for measuring parameters related to gas movement, such as gas pressure and permeability. Gas pressure can be measured with U-tube manometers containing different fluids, such as water or mercury. Such manometers generally measure differential pressure because one end of the tube is inserted into soil or rock and the other is exposed to the atmosphere. Manometers can be inclined to increase sensitivity. Pressure transducers are used widely to measure absolute or differential gas pressure. The operational range of these instruments varies, and their precision is generally a percentage of the full-scale measurement range. Manufacturers include Setra (Acton, Massachusetts) and Microswitch Honeywell (Freeport, Illinois). Because transducers are subject to drift, they have to be calibrated periodically. Data can be recorded automatically in a data logger.

Gas permeability can be measured in the laboratory on undisturbed or repacked cores. Repacking should be done only on samples having low clay content. Because repacking changes structure, gas transport parameters are affected. The more structured the soil, the bigger the potential change. Clay soils tend to be more structured. Permeability measurements include determination of flow rate of each phase under an applied pressure gradient and measurement of saturation in unsaturated systems (Scheidegger, 1974). Various methods used to measure air and water permeabilities include those in which both phases move and are measured at the same time and those in which the permeability of one fluid phase is measured while the other phase remains stationary. Steady-state methods that hold the wetting phase stationary are used most widely (Corey, 1986). Tempe cells (Soilmoisture Equipment Corp., Santa Barbara, California) used for measuring water retention functions can be adapted as permeameters and include a sample holder with ceramic end plates. Alternatively, if sample shrinkage is expected, flexible wall permeameters can be used to minimize air flow along the annulus between the sample and the holder. Sharp et al. (1994) described an electronic minipermeameter for measuring gas permeability in the laboratory. Gas is injected at a constant pressure and the steady-state flow is measured by electronic mass flow transducers. Permeabilities can be measured over a wide range (10^{-15} to 10^{-8} m^2). The Hassler method (Hassler, 1944) controls the capillary pressure at both ends of a soil core by means of capillary barriers and measures air and water relative permeabilities at the same time under a pressure gradient. The capillary barriers separate wetting and nonwetting phases. The Hassler method was used by Stonestrom (1987) and by Springer (1993). Other procedures for laboratory measurement of gas permeability were described in Springer et al. (1995) and Detty (1992). Darcy's law is used to estimate gas permeability:

$$k_G(S_G) = -\left(J_G \mu_G\right) / (dP / dz) \qquad [8.48]$$

Additional equipment required for gas permeability measurements includes a pressure transducer or manometer, a flow sensor such as a soap film bubble meter, and a temperature sensor such as a thermistor. Gas permeabilities are measured at different gas saturations or water contents. If the sample is initially saturated with water, a minimum pressure must be reached (air entry pressure) before a continuous gas phase is achieved. Gas permeability increases as water content decreases.

The Klinkenberg b parameter can be estimated by plotting gas permeabilities measured at different mean pressures ($\overline{P}$) as a function of the reciprocal mean pressure at which the tests were performed (Equation [8.38]). Rearranging Equation [8.38] results in:

$$k_G = k\left(1 + b_i / \overline{P}\right) = k + kb_i(1 / \overline{P}) \qquad [8.49]$$

Therefore, the slope is the product of k times b_i and the intercept is the true permeability.

Gas diffusivities can be measured in open, semi-open and closed systems (Abu-El-Sha'r, 1993). An open system involves component gases flowing past the edges of the soil. Pressure gradients and absolute pressures can be controlled by regulating the flow rate of the component gases. A semi-open system is generally termed a Stefan tube that consists of the diffusing substance in liquid form at the base and either free air (if measuring free-air diffusivity) or the porous medium (if measuring effective diffusivity of the porous medium) at the top. Closed systems generally consist of two chambers connected by a capillary or chamber filled with the porous medium (Glauz and Rolston, 1989). This system can be used in the study of noxious gases. Semi-open systems are generally used in hydrology to measure effective binary diffusion coefficients. Fick's law is generally used to analyze these experiments. Although most studies in the past used nonequimolar pairs of gases, none of these studies considered nonequimolar diffusion. Experiments conducted by Abu-El-Sha'r (1993) were the first to use an equimolar pair of gases (N_2 and CO) to determine effective binary molecular diffusion coefficients. Details of various procedures for measuring molecular diffusion coefficients are outlined in Rolston (1986).

Single-gas experiments are used to measure the Knudsen diffusion coefficient by applying the dusty gas model (Abu-El-Sha'r, 1993):

$$N_i^T = -\left(\frac{D_i^k}{RT} + \frac{\overline{P}k}{\mu_G RT} \right)\nabla P \qquad [8.50]$$

Rearranging Equation [8.50] results in:

$$N_i^T = -\left(\frac{D_i^k \mu_G}{\overline{P}} + k \right)\frac{\overline{P}}{\mu_G RT}\nabla P \qquad [8.51]$$

Plotting $N_i^T LRT / \Delta P$ versus $\overline{P}$ should result in a straight line with an intercept of D_i^k and a slope of k / μ_G, where L is the length of the column in the experiment (Abu-El-Sha'r, 1993).

8.4.3 FIELD TECHNIQUES

8.4.3.1 Estimation of Gas Permeability for Advective Gas Flow

Advective transport of gases depends on gas permeability and pressure gradient. Gas permeability can be estimated from (1) analysis of atmospheric pumping data, (2) pneumatic tests, or (3) measurements by air minipermeameters. Comparison of gas permeabilities from laboratory and field indicates that field derived estimates of gas permeabilities generally exceed laboratory derived estimates by as much as orders of magnitude (Weeks, 1978; Edwards, 1994). These differences in permeability are attributed primarily to the increase in scale from laboratory to field measurements and inclusion of macropores, fractures and heterogeneities in field measurements. Field permeability measurements in low permeability media include the effects of viscous slip and Knudsen diffusion.

8.4.3.2 Analysis of Atmospheric Pumping Data

Comparison of temporal variations in gas pressure, monitored at different depths in the unsaturated zone, with atmospheric pressure fluctuations at the surface can be used to determine minimum vertical air permeability between land surface and monitoring depth (Weeks, 1978; Nilson et al., 1991). Differential pressure transducers are used to monitor gas pressures in the unsaturated zone. Gas ports generally consist of screened intervals in boreholes of varying diameter. Flexible tubing (Cu or nylon) connects the gas port at depth with a differential pressure transducer at the surface.

One port of the transducer is left open to the atmosphere. Atmospheric pressure is monitored at the surface by a barometer.

   Data analysis consists of expressing the variations in atmospheric pressure as time harmonic functions. The attenuation of surface waves at different depths in the unsaturated zone provides information on how well or poorly unsaturated sections are connected to the surface. The accuracy of the results increases with the amplitude of the surface signals. Pressure fluctuations resulting from irregular weather variations change by as much as 20 to 30 mbar (2,000 to 3,000 Pa) during a 24-h period (Massmann and Farrier, 1992).

   If the surface pressure (upper boundary condition) is assumed to vary harmonically with time, and the water table or a low-permeability layer acts as a no-flow boundary, an analytical solution can be derived (Carslaw and Jaeger, 1959, in Nilson et al., 1991). Pneumatic diffusivity can be estimated graphically by means of the amplitude ratio. The ratio of the amplitude at a certain depth z compared with the amplitude at the surface can be obtained graphically or by time-series analysis (Rojstaczer and Tunks, 1995). Air permeability is estimated from the pneumatic diffusivity by dividing by the volumetric air content.

EXAMPLE 8.1   Estimation of gas conductivity using subsurface attenuation of barometric pressure fluctuations

The use of barometric pressure fluctuations to estimate subsurface gas conductivity is demonstrated with data from the Hanford Nuclear Reservation in the Columbia Plateau of south-central Washington state. The depth to the water table at the site is 66 m. The stratigraphy in the unsaturated zone consists of about 38 m of permeable sand and gravel, underlain by an 8-m thick caliche layer, and a 20-m thick gravel layer to the water table.

   The average barometric pressure at the Hanford Nuclear Reservation is approximately 100,2144 Pa. Fluctuations in barometric pressure cause vertical pressure gradients in subsurface gases, as shown in Diagram 8.1.1. These data are from a stainless-steel, 15-cm diameter well with a single-screened interval from 52.5 to 56.6 m which is beneath the caliche layer. Pressure differentials, defined as subsurface pressure minus barometric pressure, are on the order of 1,000 Pa in this deeper layer.

   Pressure attenuation and phase shift at a given frequency can be used to infer subsurface vertical gas conductivity. The calculated conductivity reflects the lowest conductivity in the section, which is the caliche layer in this section. A low-pass filter and a Fourier transform were applied to isolate diurnal and cyclonic periods (Diagrams 8.1.2 and 8.1.3). A 24-h period results in an attenuation of 0.24 and a 205-h period results in an attenuation of 0.70.

$$\frac{P - P_0}{\Delta P}$$

   Nilson et al. (1991) described how to calculate the gas conductivity from the amplitude ratio $((P - P_0)/\Delta P)$ assuming the medium is homogeneous and gas flow can be described by Equation [8.31] and that the surface pressure varies harmonically as $P = P_0 + \Delta P e^{i\omega t}$:

$$\frac{P - P_0}{\Delta P} = \frac{\cosh \lambda \sqrt{i}\left(1 - \dfrac{z}{L}\right)}{\cosh \lambda \sqrt{i}} e^{i\omega t}$$

QAc9312c
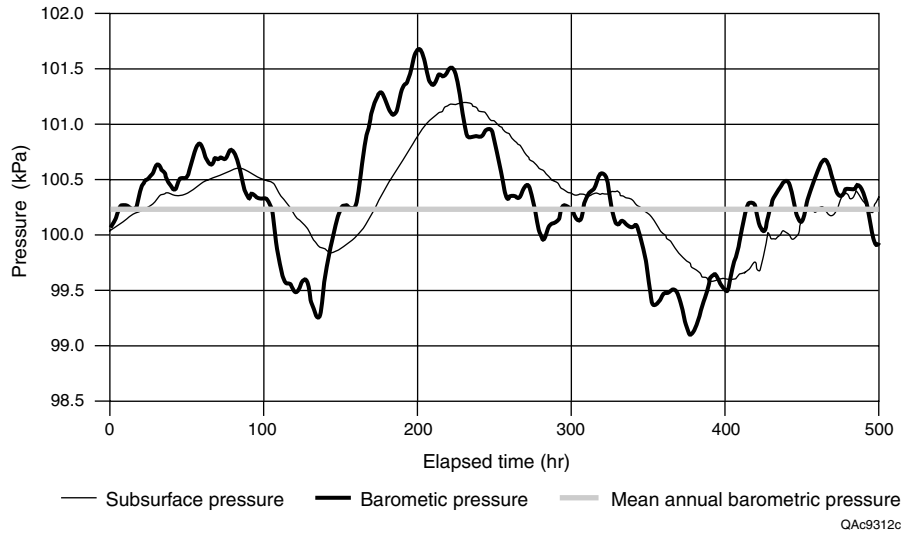
DIAGRAM 8.1.1 Surface and subsurface pressure variations. Reprinted by permission of Ground Water. Copyright 1999.

QAc9313c
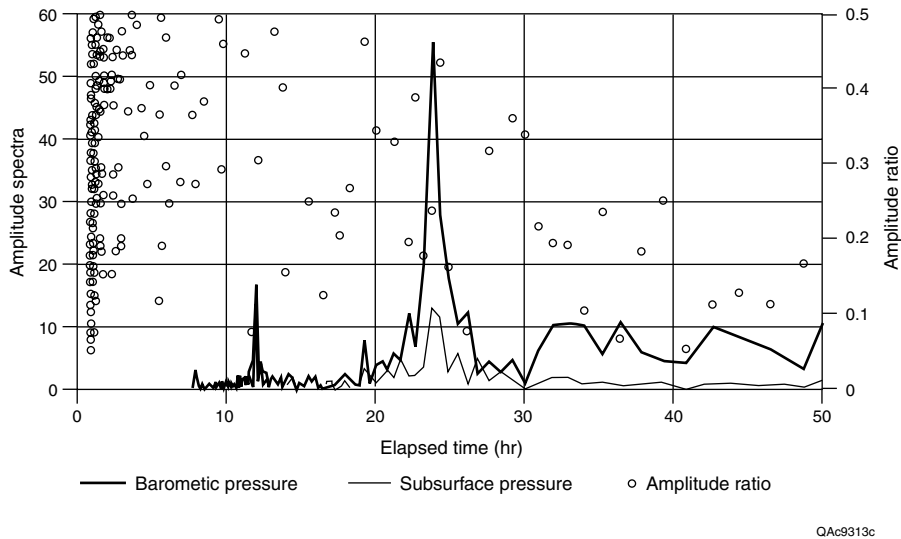
DIAGRAM 8.1.2 Pressure variations in the frequency domain (daily pressure variations).

where $\lambda = L\sqrt{\dfrac{\omega}{\alpha}} = \left[\dfrac{2\pi}{\alpha T / L^2}\right]^{1/2}$, $\sqrt{i} = (1+i)/\sqrt{2}$, z/L is the fractional depth, α is the pneumatic diffusivity $(k_G P_0)/(\phi \mu_G)$, ϕ is the volumetric gas content, μ_G is the gas viscosity, $T = 2\pi/\omega$ is the period of the pressure disturbance, and ω is the angular frequency. The caliche layer is the likely source of attenuation and barometric pressure boundary conditions are applied to the top of this layer. Therefore, the fractional depth is based on the caliche layer:

$$z/L = (52.5 - 38)/(66 - 38) = 0.518$$

DIAGRAM 8.1.3 Pressure variations in the frequency domain (cyclonic pressure variations).

The amplitude ratio and the fractional depth are used to calculate λ which is then used to calculate α. Once α has been determined, the gas permeability can be calculated by inserting a value for the volumetric gas content (0.15 for the caliche layer). The gas conductivity can then be calculated according to Equation [8.32]. The diurnal signal results in an amplitude ratio of 0.24 and a conductivity of 0.73×10^{-5} cm s^{-1}, whereas the cyclonic signal (205 hr) results in an amplitude ratio of 0.70 and a gas conductivity of 0.41×10^{-5} cm s^{-1}. These values are similar to that calculated by calibration of a numerical model (8×10^{-6} cm s^{-1} (Ellerd et al., 1999).

8.4.3.3   Pneumatic Tests

Pneumatic tests are also used widely to evaluate gas permeability in the unsaturated zone. In these tests, air is either injected into or extracted from a well and pressure is monitored in gas ports installed at different depths in surrounding monitoring wells (Figure 8.4). A reversible air pump is used to inject or extract air. Most analyses of pneumatic tests assume that the gas content (θ_G) is constant over time, i.e., that no redistribution of water occurs during the test. To evaluate this assumption, injection or extraction tests should be conducted at several different rates. If results from the different rates are similar, the assumption of constant gas content is valid. The tests can be conducted in horizontal or vertical wells.

A variety of techniques are available for analyzing pneumatic tests. The initial transient phase of the test or the steady-state portion of the test can be analyzed. If transient data are available, volumetric gas content can also be estimated. Analysis of pneumatic tests resembles the inverse problem in well hydraulics, where permeabilities are estimated from pressure data. Solutions for estimating gas permeability differ in terms of the boundary conditions that are assumed at the ground surface (such as unconfined, leaky confined and confined) and the method of solution. The lower boundary is generally assumed to be the water table or an impermeable layer. All solutions assume radial flow to a vertical well.

As discussed previously, the gas flow equation is nonlinear because of the pressure dependence of the density, viscosity and permeability (Klinkenberg effect). In many cases the pressure dependence of the density is approximated by ideal gas behavior (Equation [8.17]). Under low to moderate pressures and pressure gradients typical of unsaturated media, pressure dependence of the viscosity
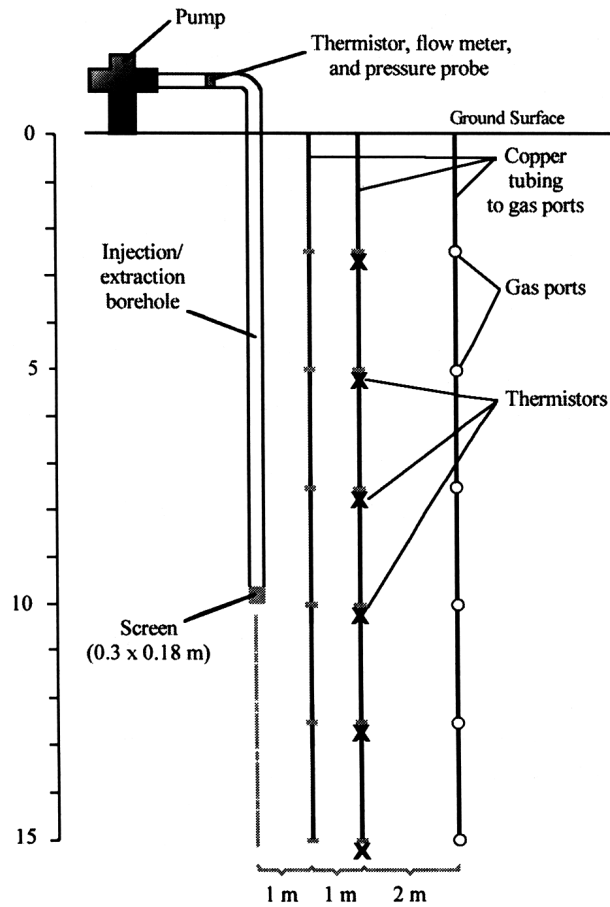
FIGURE 8.4 Schematic design for a field pneumatic test.

can be neglected. In most analyses, the Klinkenberg effect is also neglected (Massmann, 1989; Baehr and Hult, 1991). If pressure variations are assumed to be small, the transient gas flow Equation [8.52] can be written in a form similar to that of the groundwater flow Equation [8.53]:

$$\frac{\theta_G \mu_G}{P_0} \frac{\partial P}{\partial t} = \nabla(k_G \nabla P) \qquad [8.52]$$

$$S_s \frac{\partial h_w}{\partial t} = \nabla(K_w \nabla h_w) \qquad [8.53]$$

where S_s is specific storage, h_w is hydraulic head (L) and K_w is hydraulic conductivity (L t^{-1}).

A summary of various techniques for evaluating field-scale pneumatic tests is provided in Table 8.6. Massmann (1989) used many techniques developed for groundwater hydraulics to analyze transient gas tests and used a modified Theis solution for systems with no leakage from the ground surface and a modified Hantush solution for systems with leakage. The computer software AQTE-SOLV (Duffield and Rumbaugh, 1989) was used to estimate the parameters according to the Marquadt nonlinear least squares technique. Johnson et al. (1990a) developed an analytical model to evaluate transient (1-D) radial flow in a homogeneous, isotropic flow field. McWhorter (1990) developed an analytical model to analyze transient flow in a 1-D, radially symmetrical flow field

TABLE 8.6
Various approaches for evaluating field scale pneumatic tests (modified from Massmann and Madden, 1994).

Approach	Transient or steady state	No. of dimensions	Layered or homogeneous	Anisotropic or isotropic	Data
Massmann (1989)	transient	1-D	layered	anisotropic	data
Johnson et al. (1990a,b)	transient	1-D	homog.	isotropic	data
McWhorter (1990)	transient	1-D	homog.	isotropic	data
Baehr and Hult (1991)	steady state	2-D	layered	anisotropic	data
Shan et al. (1992)	steady state	2-D	homog.	anisotropic	no data
Croise and Kaleris (1992)	steady state	2-D	layered	anisotropic	data
Massmann and Madden (1994)	transient	2-D	layered	isotropic	data*

* includes horizontal wells; all other studies do not include horizontal wells.

that includes the nonlinear effects of compressible flow. He found that the nonlinear effects resulting from the pressure dependence of permeability were negligible for pressures within ±20% of P_0.

The transient phase of gas tests is generally short (approximately seconds to hours) (Edwards, 1994), and it is sometimes difficult to collect reliable data. Many studies analyze the steady-state portion of the pneumatic test. Baehr and Hult (1991) developed analytical solutions for steady-state, 2-D, axisymmetric gas flow to a partially screened well for an open system and a leaky confined system. Analysis of the leaky confined system required a Hantush type leakage term. A computer code (AIR2D) is available that includes these analytical solutions (Joss and Baehr, 1997). Falta (1995) developed analytical solutions for steady-state and transient gas pressure and stream function fields using parallel horizontal injection and extraction wells where the ground surface is open to the atmosphere. Shan et al. (1992) also developed an analytical solution for steady-state flow in homogeneous and anisotropic media that includes the effects of leakage. A constant pressure upper boundary is used that assumes that the system is completely open. Horizontal and vertical gas permeabilities are estimated using type curves. Kaluarachchi (1995) developed an analytical solution for 2-D, axisymmetric flow with anisotropic gas permeability that includes the Klinkenberg effect. Errors resulting from neglecting the Klinkenberg effect are highest in low permeability materials and near the well. Edwards (1994) used a numerical model of steady-state, radial and vertical, anisotropic, heterogeneous compressible flow with an optimization routine to estimate gas permeabilities. All tests reached steady state before 5 s (Edwards, 1994). Results of this analysis indicate that vertical heterogeneities were significant. Variations in gas permeabilities with depth were therefore attributed to increases in water content with depth. Test data can also be analyzed by means of groundwater flow models such as MODFLOW with preprocessing (Joss and Baehr, 1995), which is discussed in Section 8.5.

8.4.3.4 Air Minipermeameters

A minipermeameter is a device for measuring gas flow that is used to determine permeability in the field at a localized scale. Measurements are made rapidly and are nondestructive. A mechanically based field minipermeameter was described by Goggin et al. (1988). Compressed N_2 is injected at a constant pressure through a tip pressed against the measurement surface. The steady-state flow rate is measured by a series of rotameters, and the gas injection pressure is measured at the tip seal. The flow rate at a particular injection pressure is calibrated against measurements on core plugs of known permeability.

8.4.3.5 Evaluation of Diffusive Transport Parameters

Knudsen diffusion coefficients are measured in the laboratory using single gas experiments (Section 8.4.2), while the effective molecular diffusion coefficient can be determined from field experiments (Raney, 1949; McIntyre and Philip, 1964; Lai et al., 1976; Rolston, 1986). The simplest method for measuring gas diffusivity in near surface soils involves inserting a tube into the soil surface and supplying gas from a chamber over the inserted tube (McIntyre and Philip, 1964; Rolston, 1986). Gas diffusivity can be calculated by measuring initial gas concentration in the soil and chamber and gas concentrations in the chamber at different times. An independent measurement of volumetric gas content in the soil is also required. If gas samplers are installed at different depths in the soil and the gas concentration gradient is calculated, gas flux can be estimated by using information on the diffusivity and gas concentration gradient in conjunction with Fick's law. Kreamer et al. (1988) used atmospheric fluorocarbons to determine field tortuosities. A permeation device was used that slowly released fluorocarbon gases, the concentrations of which were monitored for several days. Nicot (1995) used instantaneous release of a tracer and continuous monitoring of gas concentration to determine field tortuosities. The data resulting from the tracer tests can be evaluated by analytical or numerical methods.

Carslaw and Jaeger (1959) presented a derivation of an analytic solution for diffusion in an isotropic, homogeneous and infinitely porous medium. The partial differential equation reduces to:

$$\frac{\partial C}{\partial t} = D_e \frac{\partial^2 C}{\partial r^2} + D_e \frac{2}{r} \frac{\partial C}{\partial r} \qquad [8.54]$$

where C is the concentration (M L^{-3}), D_e is the effective diffusion coefficient, and r is the radial distance (L). The solution to the above equation, based on instantaneous release of mass M at a point source, is:

$$C = \frac{M}{8(\pi D_e t)^{3/2}} \exp\left(-\frac{r^2}{4D_e t}\right) \qquad [8.55]$$

where M is the molecular mass (M). The inverse problem is solved by estimating effective diffusion coefficients from the measured concentration data, a procedure similar to the one described for permeability estimation.

8.5 APPLIED NUMERICAL MODELING

8.5.1 Single Phase Flow

A summary of the various types of codes available for simulating gas flow is provided in Table 8.7. Most numerical simulations of water flow in unsaturated media have generally ignored the gas phase by assuming that the gas is at atmospheric pressure. The equation that is solved is the Richards equation, which describes a single-phase (liquid), single-component (water) system. The Richards approximation is generally valid for most cases of unsaturated flow (Chapters 3 and 4).

A variety of numerical models have been developed to simulate gas flow in unsaturated systems. An important consideration in choosing a code for evaluating gas transport is the assumptions of each code. Groundwater flow models can be used to simulate gas flow in cases where the vapor behaves as an ideal gas and where pressure fluctuations are small and gas content is constant (no water redistribution) (Massmann, 1989). Such assumptions are generally valid for vapor extraction remediation systems. The code most widely used to simulate groundwater flow is MODFLOW

TABLE 8.7
Summary of types of codes available to simulate gas flow.

Code	Dim.	No. Phases	Components	Energy Balance	Porous/Fractured Systems
AIR3D	3	1	gas	no	porous
BREATH	1	2	water	yes	porous
SPLaSHWaTr	1	2	water	yes	porous
UNSAT-H	1	2	water	yes	porous
Princeton Code	2	2	water and air	no	porous
FEHM	3	2	water and air	yes	porous/fractured
TOUGH	3	2	water and air	yes	porous/fractured
STOMP	3	3	water, air, NAPL	yes	porous/fractured

(McDonald and Harbaugh, 1988). Joss and Baehr (1995) developed a sequence of computer codes (AIR3D) adapted from MODFLOW to simulate gas flow in the unsaturated zone. The codes can be used to simulate 3-D air flow in a heterogeneous, anisotropic system including induced air flow in dry wells or trenches. Pre- and postprocessors are included. AIR3D can also be used to simulate natural advective air transport in response to barometric pressure fluctuations in shallow, unsaturated systems when gravity and temperature gradients can be neglected. AIR3D transforms the air flow Equation [8.52] into a form similar to the groundwater flow Equation [8.53] that is solved by MODFLOW. Air compressibility is approximated by the ideal gas law. The simulations can be conducted (1) in a calibration mode to evaluate parameters such as permeability from pneumatic tests or (2) in a predictive mode.

8.5.2 TWO-PHASE FLOW (WATER AND AIR)

Codes have also been developed to simulate two-phase (liquid and gas), two-component (water and air) systems. In situations where the air phase retards infiltration of the water phase, a two-phase code is required (Touma and Vauclin, 1986). Two-phase codes are also required to simulate transport of volatile organic compounds. Various approaches have been developed to simulate two-phase flow. In the petroleum industry, Buckley and Leverett (1942) developed an approach that excluded the effects of capillary pressure and gravity. The basic theory of Buckley and Leverett (1942) was extended by Morel-Seytoux (1973) and Vauclin (1989). If the fluids are considered incompressible, the 1-D pressure equation reduces to (Celia and Binning, 1992):

$$q_w + q_a = constant \qquad [8.56]$$

where q_w is the water flux and q_a is the air flux. Only one equation, therefore, has to be solved. The fractional flow equation was solved by Morel-Seytoux and Billica (1985) using a finite difference approximation. Because for 2-D flow both the pressure and saturation equations must be solved, the problem no longer reduces to one equation.

Celia and Binning (1992) developed a finite element, 1-D code that considers dynamic coupling of the gas and water phases. The code is inherently mass conservative because the mixed formulation is used: temporal differentiation in terms of water content and spatial differentiation in terms of pressure head. The code was used to simulate laboratory two-phase flow experiments conducted by Touma and Vauclin (1986). The results of these simulations were compared with those achieved by means of a finite element, two-phase flow code developed by Kaluarachchi and Parker (1989) that uses the traditional h-based formulation and a finite difference code that was based on fractional flow theory used by Morel-Seytoux and Billica (1985). The simulations were used to evaluate the

conditions under which water flow is significantly altered by air flow. Infiltration experiments in a bounded column that resulted in ponded conditions showed significantly altered water flow because the air could not readily escape. An important insight gained from these simulations was that the reduction in water velocity resulted from a reduction in hydraulic conductivity with increased air content, rather than from a buildup of air pressure ahead of the wetting front (Celia and Binning, 1992).

More general codes have been developed by the National Laboratories to simulate multiphase flow and transport. TOUGH (Transport of Unsaturated Groundwater and Heat) is a 3-D code that simulates nonisothermal flow and transport of two fluid phases (liquid and gas) and two components (water and air) (Pruess, 1987). Subsequent upgrades include ATOUGH, VTOUGH, CTOUGH, ITOUGH (Finsterle and Pruess, 1995) and TOUGH2 (Pruess, 1991). A separate module has been developed for simulating transport of volatile contaminants (T2VOC). FEHM (Finite Element transport of Heat and Mass) is a 3-D, nonisothermal code that simulates two-phase flow and transport of multiple components (Zyvoloski et al., 1996). Both TOUGH and FEHM are used for simulation of flow and transport in variably saturated fractured systems at Yucca Mountain, Nevada, the proposed high-level radioactive waste disposal site. STOMP (Subsurface Transport Over Multiple Phases) simulates nonisothermal flow and transport in porous media (White and Oostrom, 1996). STOMP was developed specifically to evaluate remediation of sites contaminated by organics and includes a separate NAPL phase. Both TOUGH and STOMP use an integrated finite difference method to solve mass- and energy-balance equations.

There has been considerable interest in simulating flow in fractured systems because the proposed high-level nuclear waste facility will be located in fractured tuff. Mathematical models for simulating flow in fractured media can be subdivided into continuum and discrete fracture models (Rosenberg et al., 1994; NRC, 1996). In addition, models can be deterministic or stochastic. Continuum models can be further subdivided into equivalent continuum, dual porosity and dual permeability models (Rosenberg et al., 1994). In equivalent continuum models the system is described by a single equivalent porous medium with average hydraulic properties. This approach is considered valid if transport between fractures and matrix is rapid relative to transport within fractures (Pruess et al., 1990). Dual porosity models consider the fractures and the matrix as two interacting media with interaction between the fractures and the matrix restricted to a local scale (Pruess and Narasimhan, 1985). There is no continuous flow in the matrix. Dual porosity models are generally used to simulate transient flow and transport in saturated zones. Dual permeability models allow continuous flow in either the fractures or the matrix and an interaction term is used to describe coupling between the two media. The dual permeability formulation is generally used to simulate transient flow and transport in unsaturated systems. Dual porosity and dual permeability models treat fractures as high permeability porous media (Rosenberg et al., 1994). Discrete fracture network models assume that the matrix is not involved in flow and transport and that fluid flow can be predicted from information on the geometry of the fractures and the permeability of individual fractures (NRC, 1996). Stochastic simulation is generally used to produce several realizations of the fracture system.

8.6 APPLICATIONS OF GAS TRANSPORT THEORY

8.6.1 Soil Vapor Extraction

A detailed review of various issues related to soil vapor extraction is provided in Rathfelder et al. (1995). Soil vapor extraction has become the most common innovative technology for treating subsurface soils contaminated by volatile and semivolatile organic compounds (U.S. EPA, 1992). This popularity is partly due to its low cost relative to other available technologies, especially when contamination occurs relatively deep below the ground surface. Vapor extraction systems are also attractive because mitigation is completed *in situ,* reducing the exposure of onsite workers and the

offsite public to chemical contaminants. Vapor extraction also offers flexibility in terms of installation and operation. This flexibility allows systems to be installed at locations crowded by existing structures, roadways and other facilities and to be readily adjusted during the course of remediation to improve mass removal efficiency.

Vapor extraction involves two major processes: mass transfer and mass transport. Mass transfer is the movement from one phase to another at a particular location. Volatile and semivolatile compounds will enter the vapor phase by desorption from the soil particles through volatilization from the soil water and by evaporation from nonaqueous phase liquids (NAPLs), such as gasoline or liquid solvents. The rate at which this mass transfer occurs depends on subsurface temperature, humidity and pressure; the properties of the contaminant, including vapor pressure and solubility; and the sorptive properties of the soil.

The second major process involved in vapor extraction is mass transport, the movement of vapor from one location to another. This transport, which is primarily due to advection, is caused by pressure gradients that are developed by using extraction wells or trenches. In some instances, mass transport is enhanced through passive or active injection wells and trenches and through low permeability soil covers and cutoff walls. The rate at which mass transport occurs is a function of the distribution of soil permeabilities, soil moisture content and pressure gradients induced through the extraction and injection systems. In highly heterogeneous systems, flow may be concentrated in high permeability layers, with flow bypassing low permeability material.

The applicability of vapor extraction at a site depends on the volatility of the contaminants and the ability to generate advective gas flow through the subsurface (Hutzler et al., 1989, Johnson et al., 1995). High volatility contaminants and uniformly high permeability soils are optimal for successful vapor extraction.

The time required to clean a particular site by means of vapor extraction depends on the amount and distribution of contaminants in the subsurface and the rates at which mass transfer and mass transport occur. It is often assumed in vapor extraction applications that mass transfer is faster than mass transport, so that local equilibrium conditions exist in terms of vapor concentrations (Baehr et al., 1989; Hayden et al., 1994). Under conditions of local equilibrium, the uncertainty in cleanup time is due primarily to uncertainties in the amount and distribution of subsurface contaminants and in the amount and distribution of air flow induced by the extraction system. The distribution of both contaminants and air flow is controlled, at least partly, by the spatial distribution of soil permeability near the spill or leak. In other cases, laboratory and field experiments indicate that mass transfer from pore water to the gas phase is rate limited (Gierke et al., 1992; McClellan and Gillham, 1992). The rate limitation has been attributed to intra-aggregate or intraparticle diffusion or bypassing of low permeability zones (Gierke et al., 1992; Travis and McGinnis, 1992).

Vapor extraction systems are most often used to treat soils that have been contaminated from leaks or spills of NAPLs that occur near the ground surface. The NAPL that is released from the spill migrates through the unsaturated soil as a separate phase. As the NAPL moves through the soil, portions are trapped within the pores by capillary forces. The amount of NAPL that is trapped is termed *residual saturation*. This residual saturation depends upon the volume and rate of the NAPL release, characteristics of the soil, and properties of the contaminant. In typical situations, between 5 and 50% of the pore space may be filled by this residual saturation (Mercer and Cohen, 1990). The spatial distribution of the residual NAPL will depend upon heterogeneities in the soil column. In general, lower permeability soils tend to trap more of the NAPL than higher permeability materials (Pfannkuch, 1983; Hoag and Marley, 1986; Schwille et al., 1988). After the contaminant has entered the subsurface, it will become partitioned among the NAPL, solid, aqueous and vapor phases. In relatively fresh spills, the major fraction of the contaminant will remain in the NAPL form.

Operation of a vapor extraction system at the spill location will induce air flow through subsurface soils. The spatial distribution of air flow in the subsurface will depend on the distribution of the soil permeability: the flow will tend to occur through higher permeability channels. As the

air flows through the subsurface, it will become saturated with contaminant vapors that evaporate from the residual NAPL. After the contaminant has volatilized, it will migrate in the vapor phase to the extraction wells.

The design and operation of vapor extraction systems are described in a variety of texts, including Hutzler et al. (1988), Baehr et al. (1989), Johnson et al. (1990a, b), Pedersen and Curtis (1991) and the U.S. EPA (1991). The simplest design consists of a single vapor extraction well. In most cases, several extraction wells are used. The radius of influence of the extraction wells is often used to design the optimal distance between extraction wells (Pedersen and Curtis, 1991). Horizontal wells are used when contamination is restricted to the shallow subsurface (Connor, 1988; Hutzler et al., 1989; Pedersen and Curtis, 1991). Air injection and passive vents may be used to increase gas flow. Many studies have shown that surface seals can greatly increase the radius of influence of the extraction well and increase the efficiency of vapor extraction systems (Rathfelder et al., 1991; 1995). Modeling of soil vapor extraction systems was reviewed by Rathfelder et al. (1995) and described in references including Massmann (1989), Gierke et al. (1992), Benson et al. (1993), and Falta et al. (1993).

EXAMPLE 8.2   Using barometric pressures to help clean contaminated soils

An example of the use of passive vapor extraction to help clean up contaminated sites is provided by the cleanup of carbon tetrachloride at the Hanford Nuclear Reservation in the Columbia Plateau of south-central Washington State that is described in Example 8.1. Barometric pressure fluctuations at this site are shown in Diagram 8.1.1.

Diagram 8.2.1 shows data that describe vapor flow and carbon tetrachloride concentration. These data were collected at the same well as those shown in Diagram 8.1.1. The data from approximately 20 to 80 h correspond to a period in which air is flowing into the formation. Approximately 400 m^3 of air entered the subsurface during this 60-h period. The concentration of carbon tetrachloride in this air is essentially zero because the air entering the well is atmospheric.

At approximately 80 h the barometric pressure decreased, and the direction of airflow was reversed. Air flowed out of the well for approximately 40 h, and approximately 500 m^3 of air exited the subsurface during this period. Although air began to flow out of the well at approximately 80 h, there was a 6-h period where carbon tetrachloride concentration within this air remained essentially zero. The 6-h lag before the carbon tetrachloride concentration began to increase was the result of relatively clean air that had entered the subsurface during the previous period of air inflow. Approximately 27 g of carbon tetrachloride was removed from the subsurface during the outflow event shown in Diagram 8.2.1.

Without a check valve, atmospheric air will flow back into the subsurface through an extraction well when barometric pressure is greater than the subsurface gas pressure. Although this does not directly compromise the integrity of the system, the introduction of ambient air to the soil may result in lower concentrations of contaminants being drawn from the soil when the flow direction reverses. This in turn will reduce mass removal rates. In typical applications, these check valves will open and close at pressure differentials of less than 50 Pa. Rohay (1996) gave examples of several designs that have been used for check valves, including use of a table tennis ball or solenoid valves that open and close in response to an electrical signal controlled by differential or absolute pressures. Simulations described in Ellerd et al. (1999) indicate that use of check valves can increase the extraction of subsurface gas by 270% at the Hanford site.

Surface covers are intended to reduce vertical flow of atmospheric air into the subsurface and to enhance horizontal flow toward the extraction well by preventing short-circuiting adjacent to extraction wells. These surface seals may also reduce the dilution of contaminant

QAc9315c
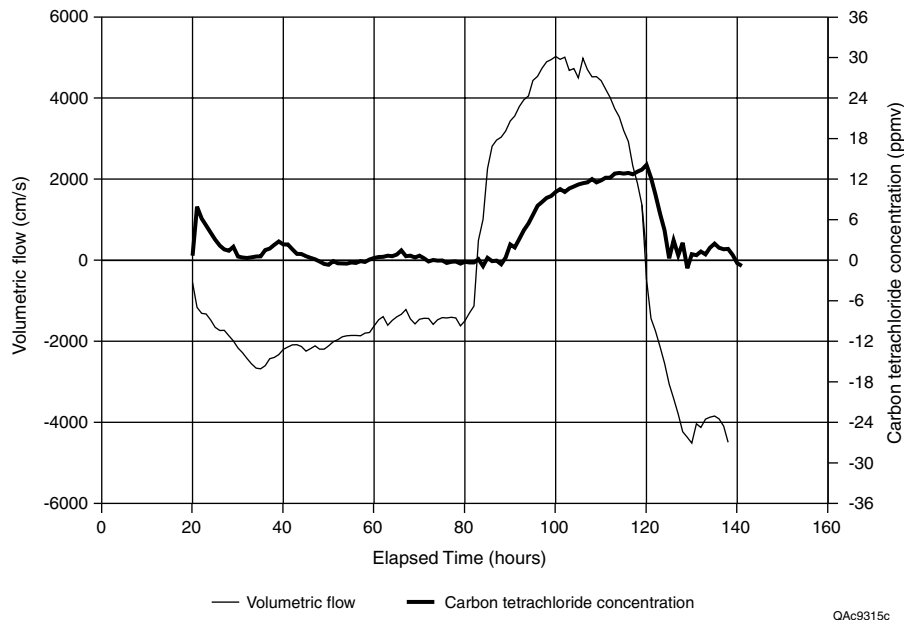
DIAGRAM 8.2.1

concentrations by preventing clean air from entering the subsurface. Surface seals would be particularly important for relatively shallow systems with permeable soils near the ground surface. By covering the ground surface with an impermeable cover, the differential between surface and subsurface gas pressure will increase for a given fluctuation in barometric pressure. Numerical simulations of covers of different radii at the Hanford site showed that volumetric flow rates more than doubled with covers of up to 90 m radius.

EXAMPLE 8.3   Case study: optimal vapor velocities for active soil vapor extraction

Most soil vapor extraction systems are operated as active systems in which pressure gradients and airflow are induced through extraction wells using mechanical blowers or pumps. The intent of active vapor extraction systems is to induce air flow through the contaminated soils. The distribution of this air flow can be conceptualized as a set of flow tubes that begin at the ground surface (or at an injection well or trench) and end at the extraction point (Diagram 8.3.1b). Clean air that is drawn into each flow tube from the atmosphere will cause NAPL to volatilize within the subsurface. If there is NAPL within the flow tube, contaminant vapors will enter the air. The maximum concentration within the vapor phase, C_S (M L^{-3}) is given by the following expression:

$$C_S = M_i P_i / RT \qquad\qquad [1]$$

where M_i is the molecular weight of gas i (M mol^{-1}), P_i is the vapor pressure for gas i (M L^{-1} t^{-2}), R is the ideal gas constant (M L^2 t^{-2} T^{-1} mol^{-1}), and T is temperature (T). Active systems should be designed based on velocities rather than pressure gradients. The optimal velocity is that which would result in saturated concentrations of volatile organics in the gas
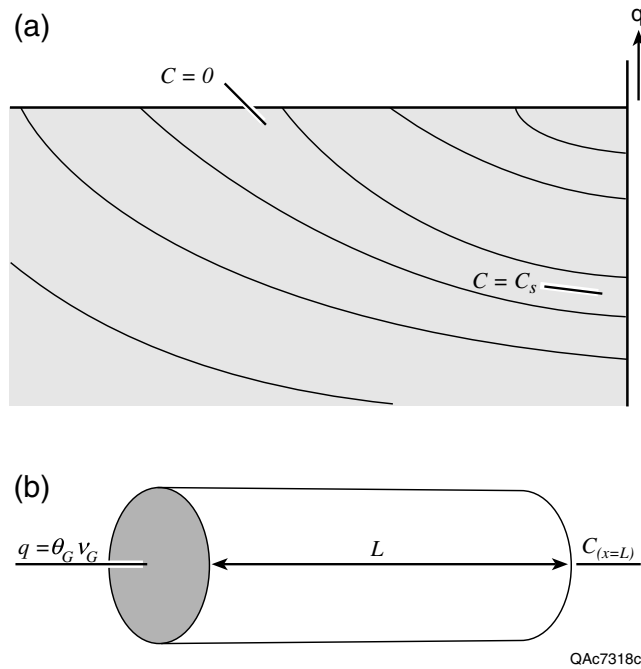
DIAGRAM 8.3.1 (a) Schematic of active vapor extraction demonstrating change in vapor concentrations as vapor moves from land surface to extraction well. (b) Detailed image of single flow tube.

phase at the well. Velocities greater than this optimal velocity would result in greater clean-up costs because more contaminated air would have to be treated. Alternatively, less-than-optimal velocities would result in longer clean-up times. Clean up progresses from the land surface to the well. The last area to be cleaned is adjacent to the well because the gas becomes saturated near the well; velocities increase near the well.

An estimate of the optimal velocity can be obtained from the following analysis that considers a one-dimensional flow tube (Figure 1a). The actual concentration in the vapor phase will approach the saturated concentration, C_S, as the air velocity within a flow tube decreases. For a flow tube with one-dimensional flow and uniform distribution of NAPL, the ratio of the effluent vapor concentration measured at the end of the tube ($C_{(x=L)}$) to the saturated vapor concentration (equilibrium concentration, C_S) is given by the following expression (Hines and Maddox, 1985):

$$\frac{C_{(x=L)}}{C^S} = 1 - \exp(-M_T^* aL / \theta_G v_G) \qquad [2]$$

M_T^* is the mass transfer coefficient (L t^{-1}), a is the contact area between liquid and gas per unit volume (L^2 L^{-3}), θ_G is the volumetric gas content, and v_G is the gas velocity. From this equation one can estimate the velocity required to reach saturation near the well. For most applications, the mass transfer coefficient and the contact area are lumped together into an effective mass transfer coefficient with units of t^{-1}.

Laboratory column experiments can be conducted to estimate the effective mass transfer coefficient, $M_T^* a$, by measuring the vapor concentration as a function of flow velocity. If it is assumed that the laboratory-derived transfer coefficient is representative of field-scale conditions, then Equation [2] can be used to select a velocity in the field based upon the

lengths of the flow tubes that are developed with the vapor extraction system. The field velocities can be approximated by calculating the flux using Darcy's law based on head measurements at two points and dividing the flux by the volumetric gas content. Gas velocities should be used as the design parameter for active soil vapor extraction systems. Because permeabilities can be highly variable, pressure decreases are not that important. Optimal velocities in one flow tube may not be optimal in another. The pumping rates should be controlled to achieve maximum saturations at the well.

8.6.2 Radon Transport

Radon transport has created considerable interest because of the radiological health hazard (lung cancer) associated with the decay products of radon. Radium radioactively decays to radon, and the greatest doses of radiation result from ^{222}Rn. Many of the issues related to radon transport were reviewed in Nazaroff (1992). Recent evaluations of contaminated sites have focused on risk assessment and suggest that one of the most critical exposures to radon and volatile organic contaminants is from movement of soil gas into buildings. Much research is therefore currently being conducted on gas movement from soil into buildings.

The typical range of radium content in surficial sediments in the United States is 10 to 100 Bq kg^{-1} (Bq, becquerel is the SI unit for activity, which corresponds to the number of atoms needed to yield a radioactive decay rate of one per second) (Nazaroff, 1992). Much higher concentrations of radon occur near uranium mines and mill tailings. Radon is also emitted from low-level radioactive waste disposal sites. The half-life of ^{222}Rn is 3.8 days. Radon partitions among solid, liquid and gas phases. Diffusive transport is sufficient to account for radon migration from unsaturated material into the atmosphere. Radon fluxes estimated on the basis of diffusion are consistent with experimental measurement (Nazaroff, 1992). The diffusion coefficient of ^{222}Rn in air is 1.2×10^{-5} m^2 s^{-1} (Hirst and Harrison, 1939). The effective diffusion coefficient, including the effect of reduced cross-sectional area and increased path length (tortuosity), is about a factor of four smaller than the free air diffusion coefficient in fairly dry soils (Nazaroff, 1992). Effective diffusivities in saturated systems are about four orders of magnitude less than those in dry soils (Tanner, 1964). This difference has been used in the design of engineered barriers for uranium mill tailings to minimize upward movement of radon into the atmosphere. Thick clay layers (0.6 to 2 m) are used as radon barriers because they retain much more water than does sand and thus reduce radon diffusion. Desiccation of clay, however, results in cracking and development of preferred pathways for gas transport. Typical diffusive fluxes for radon estimated by Nazaroff (1992) average 0.022 Bq m^{-2} s^{-1}, which is the same average as diffusive fluxes in Australian soils estimated by Schery et al. (1989).

Advection is generally considered more important than diffusion for radon transport into buildings because concrete slabs provide a barrier to diffusion and ventilation causes a pressure differential between indoor and outdoor air that drives advective gas transport. Advective gas transport, described by Darcy's law, varies with permeability and pressure gradient. Because permeability generally decreases with grain size, Nazaroff and Sextro (1989) suggested that diffusion is dominant in low permeability materials and advection dominant in high permeability materials, the cutoff being ~ 10^{-11} m^2. Gas permeability is generally anisotropic because sediment layering results in higher permeabilities horizontally than vertically. Openings in the substructures of buildings provide pathways for advective radon transport into buildings. The average indoor ^{222}Rn concentration in buildings is 50 Bq m^{-3}; in soil, ~ 30 Bq m^{-3} (Nazaroff, 1992). Pressure differentials across buildings may result from ventilation caused by open windows and doors, fans, heating and air conditioning. Heating generally increases radon entry into buildings; air conditioning reduces it.

The construction of building substructures can have important implications for advective gas transport. Concrete slabs are commonly underlain by gravel layers. Penetrations at floor wall joints

and perimeter drain systems allow gas transport. Temperature differences, barometric pressure fluctuations, wind and rain cause pressure differentials (Nazaroff, 1992).

Diffusive fluxes can account for about 10% of mean radon concentration in single family dwellings (Nero et al., 1986). Nazaroff (1992) presented several different paradigms for radon entry into dwellings. In the base case, transport of radon from the soil into buildings is attributed primarily to advective airflow driven by weather and ventilation. An alternative paradigm would be soil with strongly varying permeability, in which case diffusion would be important for transporting gas from high- to low-permeability regions, such as gravel seams or cracked clays. Another alternative is a high-permeability material at the interface between the building and the soil, such as a gravel layer or a thin air gap. In this case, molecular diffusion from the native low-permeability soil to the high-permeability gravel is important, and advection alone would result in much slower transport of radon.

8.6.3 Water Vapor Diffusion

Analysis of water vapor transport in natural systems can be done by approximating soil gas as a two-component system containing water vapor and air. Diffusion of water vapor is important in near-surface sediments where evaporation is occurring and in arid systems where water contents are extremely low. The simple theory of water vapor diffusion assumes that water vapor behaves like other gases. The flux of water vapor (water in the gas phase) is:

$$q_G^w = -\theta_G \tau D_G^w \nabla \rho_v \qquad [8.57]$$

where D_G^w is the binary diffusion coefficient for water vapor in air and ρ_v is the water vapor density. The Kelvin equation can be used to express water vapor density in terms of temperature and matric potential head:

$$\rho_v = \rho_v^0 \cdot RH = \rho_v^0 \exp \frac{h_m V_w}{\rho_w RT} \qquad [8.58]$$

where ρ_v^0 is saturated vapor density, RH is relative humidity, h_m is matric potential (Pa), V_w is the molar volume of water (1.8×10^{-5} m^3 mol^{-1}), R is the gas constant and T is Kelvin temperature. Laboratory experiments showed that water vapor fluxes estimated by Equation [8.58] underestimated measured water vapor fluxes by as much as one order of magnitude. Philip and de Vries (1957) attributed the discrepancy between laboratory measured and estimated water vapor fluxes to (1) liquid island enhancements and (2) increased temperature gradients in the air phase. Liquid island enhancement refers to the fact that when the liquid phase is discontinuous, liquid islands act as short circuits for thermal vapor diffusion. Water vapor condenses on one side of liquid water and evaporates on the other side. This results in an increased cross-sectional area for diffusion from the volumetric gas content to the sum of the volumetric gas and liquid contents (porosity) when the water phase is discontinuous. Temperature gradients in the gas phase are much higher than the average temperature gradients in porous media because thermal conductivity in the gas phase is much lower than that in the liquid and solid phases:

$$q_G^w = -\theta_G \tau_G D_G^w \left. \frac{\partial \rho_g^w}{\partial \psi} \right|_T \nabla \psi - f \frac{\nabla T_G}{\nabla T} \tau_G D_G^w \left. \frac{\partial \rho_v}{\partial T} \right|_\psi \nabla T \qquad [8.59]$$

where ∇T_G is the average temperature gradient in the gas phase, ∇T is the average bulk temperature gradient in the system, and f is a correction factor for liquid island enhancement and is equal to the porosity when the liquid phase is discontinuous (Milly and Eagleson, 1980). Thermal vapor

flux, resulting from variations in saturated vapor pressure with temperature, is generally considered much more important than isothermal vapor flux. A temperature difference of 1°C at 20°C results in a greater difference in vapor density (1.04×10^{-3} kg m^{-3}) than does a 1.5 MPa difference in matric potentials from –0.01 to –1.5 MPa (0.17×10^{-3} kg m^{-3}) (Hanks, 1992). The temperature dependence of saturated vapor pressure is given in Table 8.1. Temperature gradients are generally high in near surface sediments, and nonisothermal vapor diffusion is important.

One-dimensional liquid and vapor transport in arid and semiarid systems has been simulated by two-phase (liquid and gas), single-component (water), nonisothermal codes (BREATH, SPLaSH-WaTr, UNSAT-H) (Stothoff, 1995; Milly, 1982; Fayer and Jones, 1990). Advective gas transport is not included. In many applications of these codes, liquid and vapor flow is simulated in response to atmospheric forcing functions. Mass and energy equations are solved sequentially, and the resultant tridiagonal equations are readily solved by the efficient Thomas algorithm. These simulators solve the continuity equation for water:

$$\frac{\partial}{\partial t}\left(\rho_l^w \theta_l + \rho_G^v \theta_G\right) = -\nabla \cdot \left(\rho_l^w q_l + \rho_G^v q_v\right)$$ [8.60]

where ρ_l^w is the density of water in the liquid phase and ρ_G^v is the density of water vapor in the gas phase. Darcy's law is used to solve the liquid water flux, and the theory of Philip and de Vries (1957) is used to solve the vapor diffusive flux. The energy balance equation is also solved in these codes. Numerical simulations of liquid and vapor flux provide insights on flow processes in the unsaturated zone. Simulations in response to 1 yr of atmospheric forcing in the Chihuahuan Desert of Texas showed net downward water flux in response to seasonally varying temperature gradients that was consistent with isotopic tracer data (Scanlon and Milly, 1994). Simulations at Yucca Mountain, Nevada, evaluated the impact of hydraulic properties on infiltration (Stothoff, 1997). For low permeabilities in this system, vapor transport was dominant. The simulations demonstrated the importance of the alluvial cover on fractured bedrock in decreasing downward water flux. The UNSAT-H code was used to evaluate the performance of engineered barriers, including a capillary barrier at the Hanford site (Fayer et al., 1992). Hysteresis was found to be important in reproducing drainage measured through the capillary barrier.

8.6.4 PREFERENTIAL FLOW

Preferential flow refers to nonuniform movement of a fluid. In most cases preferential flow has been examined with respect to water flow. Preferential flow can occur in macropores that are noncapillary size pores, such as desiccation cracks in clays, worm holes and root tubules in soils, and fractures in rocks. Because macropores drain rapidly they are generally dry, and preferential flow of gases should therefore be much greater than that of liquids.

There has been much interest in fractured systems in recent years because the proposed high level radioactive waste disposal facility is located in fractured tuff. Fractures allow rapid transport of contaminants in unsaturated systems. The cubic law is used to describe fracture flow, which is proportional to the fracture aperture cubed for a given head gradient. Laminar flow between smooth parallel plates is given by:

$$Q = Aq_G = (bw)\frac{b^2}{12\mu_G}\frac{\partial P}{\partial z} = \frac{b^3 w}{12\mu_G}\frac{\partial P}{\partial z}$$ [8.61]

where Q is the volumetric flow rate (L^3 t^{-1}), b is aperture opening (L), w is the width of the fracture perpendicular to the direction of flow (L), bw is the cross-sectional area (L^2) and P is the hydraulic head (Pa) (Snow, 1968). Fractures are important because they account for most of the permeability

in the system, whereas the matrix is important because it accounts for most of the porosity. Nilson et al. (1991) evaluated contaminant gas transport in fractured permeable systems. For example, a system that has 1 mm wide fractures (δ_f) separated by 1 m slabs of matrix (δ_m) with a matrix porosity of 0.10 (ϕ_m) will have a ratio of capacitance volumes (V) as follows (Nilson et al., 1991):

$$\frac{V_m}{V_f} = \frac{\phi_m \delta_m}{\delta_f} \sim 100 \qquad [8.62]$$

Most mass flow occurs through the fractures as shown by the following (Nilson et al., 1991):

$$\frac{Q_f}{Q_m} = \frac{A_f q_f}{A_m q_m} \sim \frac{\delta_f}{\delta_m} \frac{\left(\delta_f^{\,2}/12\right)}{k_m} \sim \frac{1}{12} \frac{\delta_f^{\,3}}{\delta_m k_m} \sim 10^5 \qquad [8.63]$$

where Q is the mass flow, q is the mass flux density, and k_m is the gas permeability of the matrix (10^{-15} m^2). Even with high matrix permeability ($\sim 10^{-12}$ m^2) and narrow fractures (10^{-4} m), about 99% of the flow will occur in the fractures.

In fractured, permeable media, advective fluxes resulting from barometric pressure fluctuations may be orders of magnitude greater than diffusive fluxes and could result in upward movement of contaminated gases into the atmosphere (Nilson et al., 1991). Theoretical analyses by Nilson et al. (1991) showed that in homogeneous media, a differential barometric pressure fluctuation of 7% ($\Delta P/P_0$) would result in the upward movement of an interface between contaminated and pure gas of 20 m if the interface were 300 m deep. In contrast, in fractured systems the volume expansion of the gas is the same as that in porous media; however, gas expansion occurs primarily in the fractures and the interface moves as much as two orders of magnitude higher in the system. The conceptual model developed for upward movement of contaminants involves upward gas movement in the fractures as a result of barometric pressure fluctuations and lateral diffusion from the fractures into the surrounding matrix, which holds the contaminants at that level until the next barometric pressure fluctuation. This is a racheting mechanism for transporting gases upward. A gas tracer experiment conducted by Nilson et al. (1992) confirmed the results of earlier theoretical analyses. These experiments showed upward movement of gas tracers in a period of months from a spherical cavity (depth ~300 m) created by underground nuclear tests at the Nevada Test Site. This rapid upward movement of gases was attributed to the effects of barometric pumping in fractured tuff.

Weeks (1987; 1993) also conducted detailed studies of flow in fractured tuff at Yucca Mountain. In areas of steep topography such as at Yucca Mountain, temperature and density-driven topographic effects result in continuous exhalation of air through open boreholes at the mountain crest in the winter, as cold dry air from the flanks of the mountain replaces warm moist air within the rock/borehole system (Weeks, 1987). Wind also results in air discharge from the boreholes that is about 60% of that resulting from temperature induced density differences (Weeks, 1993). Open boreholes greatly enhance the advective air flow at this site; numerical simulations indicate that water fluxes resulting from advective air flow under natural conditions (0.04 mm yr^{-1}) are five orders of magnitude less than those found in the borehole (Kipp, 1987) and similar in magnitude to estimated vapor fluxes as a result of the geothermal gradient (0.025 to 0.05 mm yr^{-1}; Montazer et al., 1985). These processes could cause drying of fractured rock uplands and could expedite the release of gases from underground repositories to the atmosphere (Weeks, 1993).

UNITS

Pressure: 1 atm. = 760.0 mm Hg = 101.325 kPa = 1.01 bars = 10.2 m H$_2$0
Permeability: 1 darcy = 9.87×10^{-13} m^2
Viscosity: 1 Pa s = 1,000 cp

8.7 DERIVATION OF EQUATIONS

Derivation of Equation [8.30]:

$$\frac{\partial \rho_G \phi}{\partial t} = -\nabla \cdot \left(-\frac{\rho_G k_G}{\mu_G} \nabla P \right) \qquad \text{[8.64; 8.29]}$$

Assuming ϕ is constant and writing gas density in terms of pressure (Equation [8.17]):

$$\phi \frac{\partial \dfrac{PM}{RT}}{\partial t} = \nabla \cdot \left(\frac{\dfrac{PM}{RT} k_G}{\mu_G} \nabla P \right) \qquad \text{[8.65]}$$

The term M/RT is constant and can be canceled:

$$\frac{M}{RT} \phi \frac{\partial P}{\partial t} = \frac{M}{RT} \nabla \cdot \left(\frac{P k_G}{\mu_G} \nabla P \right) \qquad \text{[8.66]}$$

Assuming permeability and viscosity are constant:

$$\phi 2P \frac{\partial P}{\partial t} = \frac{k_G}{\mu_G} 2P \nabla \cdot (P \nabla P) \qquad \text{[8.67]}$$

$$\frac{\partial P^2}{\partial t} \approx \frac{k_G P_0}{\phi \mu_G} \nabla^2 P^2 \qquad \text{[8.68; 8.30]}$$

Equation [8.69] is Equation [8.30] in Section 8.2.2. The derivation assumes single-phase flow. Similar expressions can be developed for two-phase flow (air and water) by using the volumetric gas content (θ_G) instead of porosity.

Equation [8.31] is derived by assuming that the pressure fluctuations are small, an assumption satisfied in many cases in the unsaturated zone:

$$P = P_0 + \Delta P$$
$$P^2 = P_0^2 + 2\Delta P P_0 + (\Delta P)^2 \qquad \text{[8.69]}$$

The first term on the right of Equation [8.70] is a constant; therefore, its derivative is zero. The third term is negligible and is neglected. Equation [8.30] can be converted to Equation [8.31] using the following:

$$\frac{\partial P^2}{\partial t} = 2P_0 \frac{\partial P}{\partial t} \qquad \text{[8.70]}$$

$$\nabla^2 P^2 = 2P_0 \nabla^2 P$$

$$\frac{\partial P}{\partial t} = \alpha \nabla^2 P \qquad \text{[8.71; 8.31]}$$

Derivation of the form of equations (Section 8.1.6.3) for a binary gas mixture is shown in the following. Diffusive transport of nonequimolar gases in an isobaric system mixture is described by (Cunningham and Williams, 1980):

$$N_i^D = J_{iM}^m + N_i^N \qquad [8.72]$$

The molar diffusive flux of component i (N_i^D) results from the molecular diffusive flux (J_{iM}^m) and the nonequimolar diffusive flux (N_i^N) of gas component i. Because the nonequimolar diffusive flux is nonsegregative, the contribution of each species is proportional to its mole fraction x_i and Equation [8.72] can be reformulated:

$$N_i^D = J_{iM}^m + x_i N^N \qquad [8.73]$$

$$\sum_{i=1}^v N_i^D = \sum_{i=1}^v J_{iM}^m + \left(\sum_{i=1}^v x_i \right) N^N \qquad [8.74]$$

Because $\displaystyle\sum_{i=1}^v x_i = 1$, it can be proved that $\displaystyle\sum_{i=1}^v J_{iM}^m = 0$; Equation [8.74] can be rewritten as:

$$\sum_{i=1}^v N_i^D = N^N \qquad [8.75]$$

If Equation [8.73] is applied to the two components A and B of an isobaric, binary mixture, Equation [8.74] becomes:

$$N_A^D = -D_{AB}\nabla n_{AM} + x_A(N_A^D + N_B^D) \qquad [8.76]$$

$$N_B^D = -D_{BA}\nabla n_{BM} + x_B(N_A^D + N_B^D) \qquad [8.77]$$

where n_{AM} and n_{BM} are the number of moles of gases A and B. Because the system is isobaric, the total flux is zero (otherwise a pressure gradient would result), and Equations [8.76] and [8.77] reduce to Fick's law applied to the total diffusive flux. This is the only case when Fick's law is strictly valid. In deriving Equations [8.76] and [8.77], the segregative diffusive flux is assumed to follow a gradient law:

$$J_{AM}^m = -D_{AB}\nabla n_{AM} \qquad [8.78]$$

The following two equations result:

$$N_A^D = -D_{AB}\nabla n_{AM} + x_A(N_A^D + N_B^D) \qquad [8.79]$$

$$N_B^D = -D_{BA}\nabla n_{BM} + x_B(N_A^D + N_B^D) \qquad [8.80]$$

Multiplying Equation [8.79] with x_B and [8.80] with x_A results in:

$$x_B N_A^D = -x_B D_{AB}\nabla n_{AM} + x_A x_B(N_A^D + N_B^D) \qquad [8.81]$$

$$x_A N_B^D = -x_A D_{BA}\nabla n_{BM} + x_A x_B(N_A^D + N_B^D) \qquad [8.82]$$

Subtracting Equation [8.82] from Equation [8.81] results in:

$$x_B N_A^D - x_A N_B^D = -D_{AB}(x_B \nabla n_{AM} - x_A \nabla n_{BM}) \qquad [8.83]$$

Because $n_{AM} + n_{BM} = n =$ constant and $x_A + x_B = 1$, Equation [8.83] can be rewritten as:

$$x_B N_A^D - x_A N_B^D = -D_{AB}\left((1 - x_A)\nabla n_{AM} - x_A(\nabla n_{BM})\right)$$

$$x_B N_A^D - x_A N_B^D = -D_{AB}\left(\nabla n_{AM} - x_A \nabla(n_{AM} + n_{BM})\right) \qquad [8.84]$$

$$x_B N_A^D - x_A N_B^D = -D_{AB}\nabla n_{AM}$$

According to the ideal gas law $P_A = \dfrac{n_{AM}}{RT}$; therefore:

$$\frac{x_B N_A^D - x_A N_B^D}{D_{AB}} = -\frac{\nabla P_A}{RT} \qquad [8.85]$$

REFERENCES

Abriola, L.M., C.S. Fen, and H.W. Reeves. 1992. Numerical simulation of unsteady organic vapor transport in porous media using the dusty gas model, 195–202, *in Proc. of the Int. Assoc. Hydrol. Conf. on Subsurface Contamination by Immiscible Fluids*, A.A. Balkema, Rotterdam, Netherlands.

Abu-El-Sha'r, W.Y. 1993. Experimental Assessment of Multicomponent Gas Transport Mechanisms in Subsurface Systems, Ph.D. dissertation, 75, Univ. of Mich., Ann Arbor.

Abu-El-Sha'r, W.Y. and L.M. Abriola. 1997. Experimental Assessment of Gas Transport Mechanisms in Natural Porous Media: Parameter Evaluation, *Water Resour. Res.,* 33:505–516.

Alzaydi, A.A. 1975. Flow of Gases through Porous Media, 172 pp., Ohio State University, Columbus.

Alzaydi, A.A. and C.A. Moore. 1978. Combined pressure and diffusional transition region flow of gases in porous media, *AICHE J.,* 24(1):35–43.

Amali, S. and D.E. Rolston. 1993. Theoretical investigation of multicomponent volatile organic vapor diffusion: steady-state fluxes, *J. Environ. Qual.,* 22:825–831.

Amali, S., D.E. Rolston, and T. Yamaguchi. 1996. Transient multicomponent gas-phase transport of volatile organic chemicals in porous media, *J. Environ. Qual.,* 25:1041–1047.

Auer, L.H., N.D. Rosenberg, K.H. Birdsell, and E.M. Whitney. 1996. The effects of barometric pumping on contaminant transport, *J. Contam. Hydrol.,* 24:145–166.

Baehr, A.L. and C.J. Bruell. 1990. Application of the Stefan-Maxwell equations to determine limitations of Fick's law when modeling organic vapor transport in sand columns, *Water Resour. Res.,* 26:1155–1163.

Baehr, A.L., G.E. Hoag, and M.C. Marley. 1989. Removing volatile contaminants from the unsaturated zone by inducing advective air-phase transport, *J. Contam. Hydrol.,* 4:1–26.

Baehr, A.L. and M.F. Hult. 1991. Evaluation of unsaturated zone air permeability through pneumatic tests, *Water Resour. Res.,* 27:2605–2617.

Benson, D.A., D. Huntley, and P.C. Johnson. 1993. Modeling vapor extraction and general transport in the presence of NAPL mixtures and nonideal conditions, *Ground Water,* 31(3):437–445.

Bird, R.B., W.E. Stewart, and E.N. Lightfoot. 1960. Transport Phenomena, 780 pp., John Wiley, NY.

Brooks, R.H. and A.T. Corey. 1964. Hydraulic Properties of Porous Media, 27 pp., Colorado State Univ. Hydrology Paper No. 3.

Brusseau, M.L. 1994. Transport of reactive contaminants in heterogeneous porous media, *Rev. Geophys.,* 32:285–313.

Buckley, S.E. and M.C. Leverett. 1942. Mechanisms of fluid displacement in sands, *Trans. Am. Inst. Mining Metallurgical Engineers,* 146:107–116.

Burdine, N.T. 1953. Relative permeability calculations from pore size distribution data, *Petr. Trans., AIME,* 198:71–78.

Carslaw, H.S. and J.C. Jaeger. 1959. The Conduction of Heat in Solids, 510 pp., Oxford Univ. Press, London.

Celia, M.A. and P. Binning. 1992. A mass conservative numerical solution for two-phase flow in porous media with application to unsaturated flow, *Water Resour. Res.,* 28:2819–2828.

Charbeneau, R.J. and D.E. Daniel. 1992. Contaminant transport in unsaturated flow, 15.1–15.54, *in Handbook of Hydrology,* D.R. Maidment, (ed.), McGraw-Hill, Inc., NY.

Childs, S.W. and G. Malstaff. 1982. Heat and Mass Transfer in Unsaturated Porous Media, 173, Pacific Northwest Laboratory.

Collins, R.E. 1961. Flow of Fluids through Porous Media, 270 pp., van Nostrand-Reinhold, Princeton, NJ.

Connor, J.R. 1988. Case study of soil venting, *Pollution Engr.,* 20(7):74–78.

Corey, A.T. 1954. The interrelation between gas and oil relative permeabilities, *Producer's Monthly,* 19(1):38–44.

Corey, A.T. 1986. Air permeability, 1121–1136, *in* A. Klute (ed.), *Methods of Soil Analysis, Am. Soc. Agron.,* Madison, Wisconsin.

Croise, J. and V. Kaleris. 1992. Field measurements and numerical simulations of pressure drop during air stripping in the vadose zone, *in* K.U. Weger (ed.), *Subsurface Contamination by Immiscible Fluids,* A.A. Balkema, Rotterdam.

Cunningham, R.E. and R.J.J. Williams. 1980. Diffusion of Gases and Porous Media, 275 pp., Plenum, NY.

Demond, A.H. and P.V. Roberts. 1987. An examination of relative permeability relations for two-phase flow in porous media, *Water Resour. Bull.,* 23(4):617–628.

Detty, T.E. 1992. Determination of Air and Water Relative Permeability Relationships for Selected Unconsolidated Porous Materials, Ph.D. dissertation, 194 pp., Univ. Ariz., Tucson.

Duffield, G.M. and J.O. Rumbaugh, 1989. AQTESOLV aquifer test solver documentation; version 1.00, Geraghty and Miller Modeling Group, Reston, VA.

Dullien, F.A.L. 1979. Porous Media: Fluid Transport and Pore Structure, 396 pp., Academic Press, NY.

Edwards, K.B. 1994. Air permeability from pneumatic tests in oxidized till, *J. Environ. Eng.,* 120(2):329–346.

Ellerd, M., J.W. Massmann, D.P. Schwaegler, and V.J. Rohay. 1999. Enhancements for passive vapor extraction: the Hanford study, *Ground Water,* Vol. 37, 427–437.

Estes, R.K. and P.F. Fulton. 1956. Gas slippage and permeability measurements, *Trans. Am. Inst. Min. Metall. Pet. Eng.,* 207:338–342.

Falta, R.W. 1995. Analytical solutions for gas flow due to gas injection and extraction from horizontal wells, *Ground Water,* 33(2):235–246.

Falta, R.W., I. Javandel, K. Pruess, and P.A. Witherspoon. 1989. Density-driven flow of gas in the unsaturated zone due to the evaporation of volatile organic compounds, *Water Resour. Res.,* 25:2159–2169.

Falta, R.W., K. Pruess, and D.A. Chesnut. 1993. Modeling advective contaminant transport during soil vapor extraction, *Ground Water,* 31(6):1011–1020.

Fayer, M.J. and T.L. Jones. 1990. UNSAT-H Version 2.0: Unsaturated soil water and heat flow model, Pac. Northwest Lab., Richland, WA.

Fayer, M.J., M.L. Rockhold, and M.D. Campbell. 1992. Hydrologic modeling of protective barriers: comparison of field data and simulation results, *Soil Sci. Soc. Am. J.,* 56:690–700.

Finsterle, S. and K. Pruess. 1995. Solving the estimation-identification problem in two-phase flow modeling, *Water Resour. Res.,* 31(4):913–924.

Forcheimer, P. 1901. Wasserbewegung durch boden, *Zeitschrift Des Verines Deutch Ing,* 49:1736–1749.

Freeze, R.A. and J.A. Cherry. 1979. *Groundwater,* 604, Prentice Hall, NJ.

Gardner, W.H. 1986. Water content, 493–545, in A. Klute (ed.), *Methods of Soil Analysis, Part 1, Physical and Mineralogical Methods, Monograph 9,* Am. Soc. Agron., Madison, Wisconsin.

Gierke, J.S., N.J. Hutzler, and D.B. McKenzie. 1992. Vapor transport in unsaturated soil columns: Implications for vapor extraction, *Water Resour. Res.,* 28(2):323–335.

Glauz, R.D. and D.E. Rolston. 1989. Optimal design of two-chamber, gas diffusion cells, *Soil Sci. Soc. Am. J.,* 53:1619–1624.

Goggin, D.J., R.L. Thrasher, and L.W. Lake. 1988. A theoretical and experimental analysis of minipermeameter response including gas slippage and high velocity flow effects, *In Situ,* 12:79–116.

Hampton, D. 1989. Coupled heat and fluid flow in saturated-unsaturated compressible porous media, 293 pp., Colorado State University, Fort Collins, CO.

Hanks, R.J., 1992. Applied Soil Physics, 176 pp., Springer-Verlag, NY.

Hassler, G.L. 1944. Method and apparatus for permeability measurements, Patent Number 2,345,935 April 2, 1944, U.S. Patent Office, Washington, DC.

Hayden, N.J., T.C. Voice, M.D. Annable, and R.B. Wallace. 1994. Change in gasoline constituent mass transfer during soil venting, *J. Environ. Eng.,* 120:1598–1614.

Hazen, A. 1911. Discussion: dams on sand foundations, *Trans. Am. Soc. Civ. Eng.,* 73:199.

Heid, J.G., J.J. McMahon, R.F. Nielsen, and S.T. Yuster. 1950. Study of the permeability of rocks to homogeneous fluids, *in A.P.I. Drilling and Production Practice*, 230, A.P.I.

Hirst, W. and G.E. Harrison. 1939. The diffusion of radon gas mixtures, *Proc. R. Soc. London, Ser. A,* 169:573–586.

Hines, A.L. and R.N. Maddox. 1985. *Mass Transfer: Fundamentals and Applications*, 529 pp., Prentice Hall, Englewood Cliffs, NJ.

Hoag, G.E. and M.C. Marley. 1986. Gasoline residual saturation in unsaturated uniform aquifer materials, *J. Environ. Eng.,* 112(3):586–604.

Hutzler, N.J., B.E. Murphy, and J.S. Gierke. 1989. State of technology review: soil vapor extraction systems, *Final Report to U.S. EPA*, 36 pp., Hazardous Waste Engineering Research Laboratory.

Jackson, R. 1977. Transport in Porous Catalysts, Elsevier Science Publ. Co., NY.

Jaynes, D.B. and A.S. Rogowski. 1983. Applicability of Fick's law to gas diffusion, *Soil Sci. Soc. Am. J.,* 47:425–430.

Jin, M., M. Delshad, B. Dwarakanath, D.C. McKinney, G.A. Pope, K. Sepehrnoori, C. Tilburg, and R.E. Jackson. 1995. Partitioning tracer test for detection, estimation, and remediation performance assessment of subsurface nonaqueous phase liquids, *Water Resour. Res.,* 31:1201–1211.

Johnson, P.C., A.L. Baehr, R.A. Brown, R.E. Hinchee, and G.E. Hoag. 1995. Innovative Site Remediation Technology: Vol. 8 – Vacuum Vapor Extraction, American Academy of Environmental Engineers, Annapolis.

Johnson, P.C., M.W. Kemblowski, and J.D. Colthart. 1990a. Quantitative analysis for the cleanup of hydrocarbon-contaminated soils by *in situ* soil venting, *Ground Water,* 28(3):413–429.

Johnson, P.C., C.C. Stanley, M.W. Kemblowski, D.L. Byers, and J.D. Colthart. 1990b. A practical approach to the design, operation, and monitoring of *in situ* soil-venting systems, *Ground Water Monit. Rev.,* 10(2):159–178.

Joss, C.J. and A.L. Baehr. 1995. Documentation of AIR3D, an adaptation of the ground water flow code MODFLOW to simulate three-dimensional air flow in the unsaturated zone, *in U.S. Geol. Surv. Open File Rept. 94-533*, 154 pp., U.S. Geol. Survey.

Joss, C.J. and A.L. Baehr 1997. AIR2D — A computer code to simulate two-dimensional, radially symmetric airflow in the unsaturated zone, *in U.S. Geological Survey Open File Report 97-588*, 106, U.S. Geological Survey.

Jury, W.A., W.R. Gardner, and W.H. Gardner. 1991. Soil Physics, 328 pp., John Wiley & Sons, Inc., NY.

Kaluarachchi, J.J. 1995. Analytical solution to two-dimensional axisymmetric gas flow with Klinkenberg effect, *J. Envir. Eng.,* 121(5):417–420.

Kaluarachchi, J.J. and J.C. Parker. 1989. An efficient finite element method for modeling multiphase flow, *Water Resources Research,* 25(1):43–54.

Kipp, K.L.J. 1987. Effect of topography on gas flow in unsaturated fractured rock: Numerical simulation, 171–176, *in* D.D. Evans and T.J. Nicholson (eds.), *Flow and Transport Through Unsaturated Fractured Rock,* Geophys. Monog. 9, Am. Geophys. Union, Washington, DC.

Klinkenberg, L.J. 1941. The permeability of porous media to liquids and gases, 200 pp., A.P.I. Drilling and Production Practice.

Kreamer, D.K., E.P. Weeks, and G.M. Thompson. 1988. A field technique to measure the tortuosity and sorption-affected porosity for gaseous diffusion of materials in the unsaturated zone with experimental results from near Barnwell, South Carolina, *Water Resour. Res.,* 24:331–341.

Lai, S.H., J.M. Tiedje, and A.E. Erickson. 1976. *In situ* measurement of gas diffusion coefficient in soils, *Soil Sci. Soc. Am. J.,* 40:3–6.

Leffelaar, P.A. 1987. Dynamic simulation of multinary diffusion problems related to soil, *Soil Sci.,* 143:79–91.

Marshall, T.J. 1958. A relation between permeability and size distribution of pores, *J. Soil Sci.,* 9:1–8.

Mason, E.A. and A.P. Malinauskas. 1983. Gas transport in porous media: the Dusty-Gas Model, *in Chem. Engr. Monogr.*, Vol. 17, 194, Elsevier, NY.

Mason, E.A., A.P. Malinauskas, and R.B. Evans. 1967. Flow and diffusion of gases in porous media, *J. Chem. Phys.,* 46:3199–3126.

Massmann, J.W. 1989. Applying groundwater flow models in vapor extraction system design, *J. Env. Engin.,* 115:129–149.

Massmann, J. and D.F. Farrier. 1992. Effects of atmospheric pressures on gas transport in the vadose zone, *Water Resour. Res.,* 28:777–791.

Massmann, J.W. and M. Madden. 1994. Estimating air conductivity and porosity from vadose-zone pumping tests, *J. Env. Eng.,* 120(2):313–328.

McClellan, R.D. and R.W. Gillham. 1992. Vapour extraction of trichloroethylene under controlled conditions at the Borden site, *in Subsurface Contamination by Immiscible Fluids*, 89–96, A.A. Balkema, Rotterdam.

McDonald, M.G. and A.W. Harbaugh. 1988. A modular three-dimensional finite-difference ground-water flow model, *in Techniques of Water Resources Investigations*, 576 pp., USGS.

McIntyre, D.S. and J.R. Philip. 1964. A field method for measurement of gas diffusion into soils, *Aust. J. Soil Res.,* 2:133–145.

McWhorter, D.B. 1990. Unsteady radial flow of gas in the vadose zone, *J. Contam. Hydrol.,* 5:297–314.

Mendoza, C.A. and E.O. Frind. 1990. Advective-dispersive transport of dense organic vapors in the unsaturated zone: Sensitivity analysis, *Water Resour. Res.,* 26(3):388–398.

Mendoza, C.A. and T.A. McAlary. 1990. Modeling of ground-water contamination caused by organic solvent vapors, *Ground Water,* 28(2):199–206.

Mercer, J.W. and R.M. Cohen. 1990. A review of immiscible fluids in the subsurface: properties, models, characterization, and remediation, *J. Contam. Hydrol.,* 6(2):107–163.

Millington, R.J. 1959. Gas diffusion in porous media, *Science,* 130:100–102.

Millington, R.J. and J.P. Quirk. 1961. Permeability of porous solids, *Faraday Soc. Trans.,* 57(7):1200–1207.

Millington, R.J. and R.C. Shearer. 1970. Diffusion in aggregated porous media, *Soil Sci.,* 3(6):372–378.

Milly, P.C.D. 1982. Moisture and heat transport in hysteretic, inhomogeneous porous media: a matric head-based formulation and a numerical model, *Water Resour. Res.,* 18:489–498.

Milly, P.C.D. and P.S. Eagleson. 1980. The coupled transport of water and heat in a vertical soil column under atmospheric excitation, 234, Ralph M. Parsons Lab., Mass. Inst. Technol.

Montazer, P., E.P. Weeks, F. Thamir, S.N. Yard, and P.B. Hofrichter. 1985. Monitoring the vadose zone in fractured tuff, Yucca Mountain, Nevada, 439–469, *in Proc. on Characterization and Monitoring of the Vadose (Unsaturated) Zone,* National Water Well Association, Denver.

Moore, C., I.S. Rai, and J. Lynch. 1982. Computer design of landfill methane migration control, *J. Env. Eng. Div. Am. Soc. Civ. Eng.,* 108:89–107.

Morel-Seytoux, H.J. 1973. Two-phase flow in porous media, *Adv. Hydrosci.,* 9:119–202.

Morel-Seytoux, H.J. and J.A. Billica. 1985. A two-phase numerical model for prediction of infiltration: Application to a semi-infinite column, *Water Resour. Res.,* 21(4):607–615.

Mualem, Y. 1976. A new model for predicting the hydraulic conductivity of unsaturated porous media, *Water Resour. Res.,* 12(3):513–521.

Muskat, M. 1946. Flow through Porous Media, 72 pp., McGraw Hill, NY.

Nazaroff, W.W. 1992. Radon transport from soil to air, *Rev. Geophys.,* 30:137–160.

Nazaroff, W.W. and R.G. Sextro. 1989. Technique for measuring the indoor ^{222}Rn source potential of soil, *Environ. Sci. Technol.,* 23:451–458.

Nero, A.V., A.J. Gadgil, W.W. Nazaroff, and K.L. Revzan. 1986. Distribution of airborne radon-222 concentrations in U.S. homes, *Science,* 234:992–997.

Nicot, J.P. 1995. Characterization of gas transport in a playa subsurface Pantex Site, Amarillo, Texas, Master's thesis, 178 pp., The University Texas at Austin.

Nilson, R.H., W.B. McKinnis, P.L. Lagus, J.R. Hearst, N.R. Burkhard, and C.F. Smith. 1992. Field measurements of tracer gas transport induced by barometric pumping, 710–716, *in Proc. of the Third International Conference of High Level Radioactive Waste Management*, Am. Nucl. Soc.

Nilson, R.H., E.W. Peterson, K.H. Lie, N.R. Burkard, and J.R. Hearst. 1991. Atmospheric pumping: a mechanism causing vertical transport of contaminated gases through fractured permeable media, *J. Geophys. Res.,* 96(B13):21933–21948.

NRC. 1996. Rock Fractures and Fluid Flow Contemporary Understanding and Applications, 551 pp., National Academy Press, Washington, DC.

Pederson, T.A. and J.T. Curtis. 1991. Soil Vapor Extraction Technology — Reference Handbook, Office of Research and Development.

Penman, H.L. 1940a. Gas and vapor movements in the soil. I. The diffusion of vapors through porous solids, *J. Agr. Sci.,* 30:437–462.

Penman, H.L. 1940b. Gas and vapor movements in the soil. II. The diffusion of carbon dioxide through porous solids, *J. Agr. Sci.,* 30:570–581.

Pfannnkuch, H. 1983. Hydrocarbon spills, their retention in the subsurface and propagation into shallow aquifers, *Office Water Resources Technology*, 51 pp., Office of Water Resources Technology, Washington, DC.

Philip, J.R. and D.A. de Vries. 1957. Moisture movement in porous materials under temperature gradients, *Trans. AGU,* 38:222–232.

Pruess, K. 1987. TOUGH User's Guide, *NUREG/CR-4645*, 78, Nuclear Regulatory Commission, Washington, DC.

Pruess, K. 1991. TOUGH2 — A general-purpose numerical simulator for multiphase fluid and heat flow, Lawrence Berkeley Lab., Berkeley, CA.

Pruess, K. and T.N. Narasimhan, 1985. A practical method for modeling fluid and heat flow in fractured porous media, *Soc. Petrol. Engin. J.,* 25:14–26.

Pruess, K., J.S.Y. Wang, and Y.W. Tsang. 1990. On thermohydrologic conditions near high-level nuclear wastes emplaced in partially saturated fractured tuff, 1, simulation studies with explicit consideration of fracture effects, *Water Resour. Res.,* 26:1235–1248.

Raney, W.A. 1949. Field measurement of oxygen diffusion through soil, *Soil Sci. Soc. Am. Proc.,* 14:61–65.

Rathfelder, K., J.R. Lang, and L.M. Abriola. 1995. Soil vapor extraction and bioventing: Applications, limitations, and future research directions, *U.S. Natl. Rep. Int. Union Geod. Geophys. 1991–1994, Rev. Geophys.,* 33:1067–1081.

Rathfelder, K., W.W.-G. Yeh, and D. Mackay. 1991. Mathematical simulation of soil vapor extraction systems: model development and numerical examples, *J. Contam. Hydrol.,* 8:263–297.

Rohay, V.J. 1996. Field tests of passive soil vapor extraction at the Hanford Site, Washington, BHI-00766, Rev. 0, Bechtel Hanford, Inc., Richland, WA.

Rojstaczer, S. and J.P. Tunks. 1995. Field-based determination of air diffusivity using soil-air and atmospheric pressure time series, *Water Resour. Res.*, 12:3337–3343.

Rolston, D.E.. 1986. Gas diffusivity, 1089–1102, *in* A. Klute (ed.), *Methods of Soil Analysis,* Vol. 1, Am. Soc. Agron., Madison, Wisconsin.

Rolston, D.E., D. Kirkham, and D.R. Nielsen. 1969. Miscible displacement of gases through soils columns, *Soil Sci. Soc. Am. Proc.,* 33:488–492.

Rosenberg, N.D., Soll, W.E., and Zyvoloski, G.A. 1994. Microscale and macroscale modeling of flow in unsaturated fractured rock: Am. Geophys. Union, Chapman Conf. on Aqueous Phase and Multiphase Transport in Fractured Rock, 22 pp., Sept. 12–15, Burlington, VT.

Satterfield, C.N. and P.J. Cadle. 1968. Diffusion and flow in commercial catalysts at pressure levels about atmospheric, *J. Ind. Eng. Chem. Fundamentals,* 7:202.

Scanlon, B.R. and P.C.D. Milly. 1994. Water and heat fluxes in desert soils 2. Numerical simulations, *Water Resour. Res.,* 30:721–733.

Scheidegger, A.E. 1974. The Physics of Flow through Porous Media, 353 pp., Univ. Toronto Press, Toronto, 3rd ed.

Schery, S.D., S. Whittlestone, K.P. Hart, and S.E. Hill. 1989. The flux of radon and thoron from Australian soils, *J. Geophys. Res.,* 94:8567–8576.

Schwille, F., W. Bertsch, R. Linke, W. Reif, and S. Zauter. 1988. Dense Chlorinated Solvents in Porous and Fractured Media: Model Experiments, Lewis Publishers, Chelsea, MI.

Shan, C., R.W. Falta, and I. Javandel. 1992. Analytical solutions for steady state gas flow to a soil vapor extraction well, *Water Resour. Res.,* 28:1105–1120.

Sharp, J.M., L. Fu, P. Cortez, and E. Wheeler. 1994. An electronic minipermeameter for use in the field and laboratory, *Ground Water,* 32(1):41–46.

Shepherd, R.G. 1989. Correlations of permeability and grain size, *Ground Water,* 27(5):633–638.

Snow, D.T. 1968. Rock fracture spacings, openings, and porosities, *J. Soil Mech.,* 94:73–91.

Springer, D.S. 1993. Determining the Air Permeability of Porous Materials as a Function of a Variable Water Content under Controlled Laboratory Conditions, 71 pp., Univ. Calif., Santa Barbara.

Springer, D.S., S.J. Cullen, and L.G. Everett. 1995. Laboratory studies on air permeability, 217–247, *in* L.G. Wilson, L.G. Everett and S.J. Cullen (eds.), *Handbook of Vadose Zone Characterization and Monitoring*, Lewis Publishers.

Stonestrom, D.A. 1987. Co-Determination and Comparisons of Hysteresis-Affected, Parametric Functions of Unsaturated Flow: Water-Content Dependence of Matric Pressure, Air Trapping, and Fluid Permeabilities in a Non-Swelling Soil, 292 pp., Stanford University.

Stonestrom, D.A. and J. Rubin. 1989. Air permeability and trapped-air content in two soils, *Water Resour. Res.,* 25(9):1959–1969.

Stothoff, S.A. 1995. BREATH Version 1.1 — coupled flow and energy transport in porous media, Simulator description and user guide, U.S. Nucl. Reg. Comm.

Stothoff, S.A. 1997. Sensitivity of long-term bare soil infiltration simulations to hydraulic properties in an arid environment, *Water Resour. Res.,* 33:547–558.

Tanner, A.B. 1964. Radon migration in the ground: A review, 161–190, *in* J.A.S. Adams and W.M. Lowder (eds.), *Natural Radiation Environment*, Chicago Press.

Terzaghi, K. and R.B. Peck. 1968. Soil Mechanics in Engineering Practice, 729 pp., John Wiley & Sons, New York.

Thibodeaux, L.J., C. Springer, and L.M. Riley. 1982. Models and mechanisms for the vapor phase emission of hazardous chemicals from landfills, *J. Hazard. Mater.,* 7:63–74.

Thorstenson, D.C. and D.W. Pollock. 1989. Gas transport in unsaturated porous media, the adequacy of Fick's law, *Rev. Geophys.,* 27:61–78.

Touma, J. and M. Vauclin. 1986. Experimental and numerical analysis of two-phase infiltration in a partially saturated soil, *Transp. Porous Media,* 1:22–55.

Travis, C.C. and J.M. Macinnis. 1992. Vapor extraction of organics from subsurface soils — Is it effective?, *Env. Sci. Technol.,* 26:1885–1887.

U.S. EPA. 1991. Soil Vapor Extraction Technology Reference Handbook.

U.S. EPA. 1992. A Technology Assessment of Soil Vapor Extraction and Air Sparging, Office of Research and Development, Washington, DC.

van Genuchten, M.T. 1980. A closed-form equation for predicting the hydraulic conductivity of unsaturated soils, *Soil Sci. Soc. Am. J.,* 44:892–898.

Vauclin, M. 1989. Flow of water and air in soils, 53–91, *in* Theoretical and experimental aspects, *Unsaturated Flow in Hydrologic Modelling, Theory and Practice*, H.J. Morel-Seytoux (ed.), Kluwer Academic, Dordrecht, Netherlands.

Weast, R.C. 1986. CRC Handbook of Chemistry and Physics, CRC Press, Boca Raton, FL.

Weeks, E.P. 1978. Field determination of vertical permeability to air in the unsaturated zone, 41, *in U.S. G.S. Prof. Paper*, USGS.

Weeks, E.P. 1987. Effect of topography on gas flow in unsaturated fractured rock: concepts and observations, 165–170, *in* D.D. Evans and T.J. Nicholson (eds.), *Flow and Transport through Unsaturated Fractured Rock,* Geophy. Monograph 9, Am. Geophys. Union, Washington, DC, 1987.

Weeks, E.P. 1993. Does the wind blow through Yucca Mountain, 45–53, *in Proc. of Workshop V: Flow and Transport through Unsaturated Fractured Rock Related to High-Level Radioactive Waste Disposal*, D.D. Evans and T.J. Nicholson (eds.), U.S. Nucl. Reg. Comm., NUREG CP-0040.

White, M.D. and M. Oostrom. 1996. STOMP Subsurface Transport Over Multiple Phases Theory Guide, variously paginated, Pacific Northwest National Laboratory.

Zyvoloski, G.A., B.A. Robinson, Z.V. Dash, and L.L. Trease. 1996. Models and Methods Summary for the FEHM Application, 65 pp., Los Alamos National Lab., Los Alamos, NM.